

ABSTRACT

Vapor-liquid equilibrium data were determined at three isothermal conditions, 75° C, 65° C and 55° C, for the binary system benzene-n-octane using a modified Gillespie still.

The isothermal equilibrium data of the system are considered to be thermodynamically consistent as shown from the consistency test, and can be fitted over the entire concentration range by the three-constant Redlich-Kister⁽¹⁾ equation.

ACKNOWLEDGMENT

The author is indebted to Professor Benjamin C. -Y. Lu, who directed this work, for his guidance and encouragement in carrying out this research project.

The author is also very grateful to Mr. S. D. Chang for writing the computer programme and to Messrs. F. Giacobbi and J. Gasperetti for their technical assistance.

TABLE OF CONTENTS

	<u>PAGE</u>
ABSTRACT	i
ACKNOWLEDGMENT	ii
TABLE OF CONTENTS	iii - iv
LIST OF FIGURES	v - vi
LIST OF TABLES	vii
I INTRODUCTION	1
II VARIOUS METHODS FOR DETERMINATION OF VAPOR-LIQUID EQUILIBRIUM	2
III THEORETICAL ASPECTS	
- Evaluation of liquid phase activity coefficients	7
- Correlation and consistency of experimental data	18
IV EXPERIMENTAL DETAILS	
A. Materials and properties	23
B. Apparatus	23
- Equilibrium still	
- Accessory equipment with the still	26
- Equipment for quantitative analysis	27
C. Experimental Procedure	
- Test of the still	28
- Binary system benzene-n-octane	28
V RESULTS	30
VI DISCUSSION	45
VII CONCLUSIONS	48
VIII NOMENCLATURE	49
IX REFERENCES	51

	<u>PAGE</u>
X APPENDIX I	54
XI APPENDIX II	66
- Sample calculation	67
- Computer program used for the least square fit	72

LIST OF FIGURES

<u>FIGURE</u>		<u>PAGE</u>
1	Schematic diagram of the modified Gillespie equilibrium still.	24
2	Sketch of the pressure control system	25
3	Total pressure - composition diagram for the system benzene-n-octane at 75° C.	33
4	Binary x-y curve for the system benzene-n-octane at 75° C	34
5	Activity coefficients - composition diagram for the system benzene-n-octane at 75° C ..	35
6	$\ln \gamma_B/\gamma_O$ - composition diagram for the system benzene-n-octane at 75° C.	36
7	Total pressure - composition diagram for the system benzene-n-octane at 65° C. ...	37
8	Binary x-y curve for the system benzene-n-octane at 65° C.	38
9	Activity coefficients - composition diagram for the system benzene-n-octane at 65° C. ...	39
10	$\ln \gamma_B/\gamma_O$ - composition diagram for the system benzene-n-octane at 65° C.	40
11	Total pressure - composition diagram for the system benzene-n-octane at 55° C. ...	41
12	Binary x-y curve for the system benzene-n-octane at 55° C.	42
13	Activity coefficients - composition diagram for the system benzene-n-octane at 55° C. .	43
14	$\ln \gamma_B/\gamma_O$ - composition diagram for the system benzene-n-octane at 55° C.	44

<u>FIGURE</u>		<u>PAGE</u>
15	Calibration curve of Iron-Constantan thermocouple.	56
16	Calibration curve for composition - refractive index for the system benzene-n-octane at 25° C.	58
17	Liquid density of Benzene-Temperature diagram	62
18	Liquid density of n-octane - temperature diagram	64
19	Activity coefficients - composition diagram for the system benzene-n-heptane at 75° C..	65

LIST OF TABLES

<u>TABLE</u>		<u>PAGE</u>
1	Physical Properties of the Chemicals	23
2	Vapor-liquid equilibrium data for the system benzene-n-octane at 75° C., 65° C., and 55° C.	30
3	Calibration of temperature - absolute millivolts for the Iron-Constantan thermocouple	55
4	Calibration of composition - refractive index for the system benzene-n-octane at 25° C.	57
5	Second virial, cross coefficients, and molar volumes for the system benzene-n-octane at isothermal conditions 75° C., 65° C., and 55° C.	59
6	Redlich-Kister constants for the binary system benzene-n-octane at isothermal conditions 75° C., 65° C., and 55° C.	60
7	Liquid density of benzene vs. temperature	61
8	Liquid density of n-octane vs. temperature	63

CHAPTER I

INTRODUCTION

Much investigation in the field of thermodynamics of liquid solutions has been undertaken in connection with the prediction of vapor-liquid equilibrium^(2, 3).

These methods of prediction either give inaccurate results, or are suitable only for certain systems, or else involve quite a bit of tedious calculations.

Due to all these difficulties the vapor-liquid equilibrium relations can best be determined experimentally.

The experimental methods are based on the determination of the compositions of both the vapor and the liquid in equilibrium either at constant temperature or pressure.

The basic test for consistency is to apply Gibbs-Duhem equation to the data.

With simplifying assumptions many semi-empirical^(1, 4, 5, 6, 7, 8, 9, 10) equations have been derived as special forms of the Gibbs-Duhem equation.

The equation proposed by Redlich and Kister appears to be flexible and suitable for representing the vapor-liquid equilibrium data. The present work consists of determining the vapor liquid equilibrium data (x - y - P - T) for the binary system benzene-*n*-octane, at isothermal conditions of 75° C, 65° C, and 55° C, by means of a modified Gillespie still⁽¹¹⁾.

This system was chosen because the reported data at 1 atm^(12, 13) are inconsistent and no other experimental data are available. The experimental data were tested for consistency by the method proposed by Redlich and Kister⁽¹⁾.

CHAPTER II

DETERMINATION OF VAPOR-LIQUID

EQUILIBRIA

The separation of mixtures of liquids by means of fractional distillation is possible when the composition of the vapor coming from the liquid mixture is different from that of the liquid.

The relation between the vapor and the liquid composition must be known in order to compute fractional distillation relationships. Usually the former is obtained from information concerning the composition of the vapor which is in equilibrium with the liquid.

On this account a knowledge of vapor-liquid equilibrium data is usually essential for the quantitative design of a fractional distillation apparatus.

The methods for obtaining vapor-liquid equilibrium data can be considered in two main classifications:

- (1) the experimental determination
- (2) the theoretical relationship

In this work the experimental determination will be discussed.

1. Experimental determination of vapor-liquid equilibrium data

The measurement of vapor-liquid equilibrium data is not simple. A highly developed laboratory technique is, therefore, needed to obtain reliable data.

The methods for direct determination of equilibrium data can be classified into the following:

- (a) Distillation Method
- (b) Bomb Method
- (c) Dew and Bubble Point Method

(d) Flow Method

(e) Circulation Method

(27)

A. Distillation Method:

This is one of the oldest methods in which a small amount of liquid is distilled off from the boiling flask which contains a large charge.

During such distillation the composition of the distillate and the liquid in the still changes, and the samples represent average values.

This method involves an assumption, namely, that the vapor obtained by boiling a liquid is in equilibrium with the liquid.

There has been no adequate proof of this assumption.

B. Bomb Method: (15, 16, 17, 18)

In this method the liquid sample is placed in a closed evacuated vessel. It is then agitated at constant temperature until equilibrium is attained between the vapor and the liquid. Sample of the vapor and the liquid are withdrawn and analyzed.

The main disadvantage of this method, during sampling there are pressure changes which will disturb the equilibrium.

C. Dew and Bubble Point Method: (19, 20, 21, 22)

This technique consists in introducing a mixture of known composition into an evacuated container of variable volume. The system is maintained at constant temperature, and by varying the volume, the pressure is observed, at which condensation commences and is completed.

From such data, the saturation curves of the two phases at constant temperature can be plotted against composition.

The main disadvantages are that, the dew and bubble points are not sharply defined, hence they require to be made with highly refined precision instruments, and the materials used must be very pure and free from traces of gases.

D. Flow Method: (23, 24, 25)

Another method that has been widely used for the determination of vapor-liquid equilibrium data, is one which the vapor is passed through a series of vessels containing liquid of a suitable composition. The vapor entering the vessel may be of a composition somewhat different from the equilibrium vapor, but as it passes through the system it tends to approach equilibrium. It is obvious that it cannot be an exact equilibrium system because of the fact that a pressure drop is involved in passing the vapor through the system, i.e. there are pressure variations which will effect the equilibrium. There is also the danger of entrainment.

E. Circulation Method:

This is a common method for obtaining vapor-liquid equilibrium data by circulating the vapor through the system and bringing it back into contact with the liquid until no further change in the composition of the vapor and the liquid takes place.

Meanwhile they are kept separate to allow the removal of samples for analysis. This method is convenient to use in the region of moderate and low pressures.

While the apparatus appears to be simple, in actual practice it involves a number of complications:

- (1) The system must be completely leak-proof otherwise the total quantity of material will vary and the equilibrium

composition will also change.

(2) It is necessary to ensure that there is no entrainment of liquid.

This entrainment can be eliminated by using low boiling rates.

The number and variety of circulatory stills is large. Four of the most important are those of Othmer⁽²⁶⁾, Gillespie⁽¹¹⁾, Jones, Schoenborn and Colburn⁽²⁷⁾, and Ellis⁽²⁸⁾.

The Othmer still⁽²⁶⁾ recirculates only the vapor phase which is produced by boiling the liquid mixture in an insulated still. The vapor is removed, condensed and the overflow of condensate is returned to the still. An immersion heater is used to provide turbulent mixing and boiling without pumping.

The Jones still⁽²⁷⁾ operates in a similar manner. It only circulates the vapor phase, but the overflow condensate is vaporized outside the still before it is recontacted with the liquid phase contained therein.

The Ellis still⁽²⁸⁾ uses a glass spiral of several turns, which functions as the Cottrell pump, to recirculate both of the phases. The mixture distilled off from the boiling flask flows through the glass spiral and spurts on the thermometer well.

Equilibrium is assumed to have been attained as the contacted phases separate after leaving the glass spiral. The overflow condensate may or may not be vaporized before being returned to the boiling flask.

The family of Gillespie stills uses the action of Cottrell pump⁽²⁹⁾ to recirculate both of the phases. Equilibrium is assumed to have been attained as the contacted phases separate after leaving the upper end of the Cottrell pump. Temperature and pressure are measured at this point. The overflow condensate may or may not be vaporized

before being returned to the base of the Cottrell pump and contacted again with the liquid in the still.

There has long been dispute over the relative merits of the various types of stills. It arises both from theoretical considerations and the inconsistencies of the reported data. Summaries and discussions of them are given by Gillespie⁽¹¹⁾.

CHAPTER III

THEORETICAL ASPECTS

EVALUATION OF LIQUID PHASE ACTIVITY COEFFICIENTS AT LOW PRESSURES

Since the activity coefficients are related to compositions and are precisely defined thermodynamic functions, their calculation and correlation are required.

By definition:

$$\gamma_i = \frac{\hat{f}_i}{x_i f_i} \dots\dots\dots (1)$$

For the liquid phase

$$\hat{f}_i^L = \gamma_i^L x_i (f_i^\circ)^L \dots\dots\dots (2)$$

For the vapor phase

$$\hat{f}_i^V = \gamma_i^V y_i (f_i^\circ)^V \dots\dots\dots (3)$$

where the superscripts L and V denote the liquid and vapor phase respectively, and,

- \hat{f}_i = fugacity of component i in the solution
- f_i° = fugacity of pure component i at the standard state (ie. at the temperature and pressure of the solution)
- γ_i = activity coefficient of component i in the solution
- x_i = mole fraction of component i in the liquid phase.
- y_i = mole fraction of component i in the vapor phase

At equilibrium,

$$\hat{f}_i^L = \hat{f}_i^V$$

By equating equations (2) and (3) we get,

$$\gamma_i^L x_i (f_i^\circ)^L = \gamma_i^V y_i (f_i^\circ)^V$$

or
$$\gamma_i^L = \frac{y_i}{x_i} \cdot \frac{(f_i^\circ)^V}{(f_i^\circ)^L} \gamma_i^V$$

$$= \frac{y_i}{x_i} \cdot \frac{(f_i^\circ)^V/P}{(f_i^\circ)^L/P} \gamma_i^V$$

then
$$\ln \gamma_i^L = \ln \frac{y_i}{x_i} + \ln \frac{\phi_i^V}{\phi_i^L} + \ln \gamma_i^V \dots\dots\dots (4)$$

where,

ϕ_i^V = fugacity coefficient of pure component i in the vapor phase

ϕ_i^L = fugacity coefficient of pure component i in the liquid phase

P = total pressure of the system

In equation (4) we have to relate ϕ_i^V , ϕ_i^L and γ_i^V to measurable quantities such as pressure and temperature.

Firstly, we start with $\ln \phi_i^V$.

Since,

$$Z = 1 + \frac{B}{V} + \frac{C}{V^2} + \frac{D}{V^3} + \dots \quad (5)$$

where,

- Z = compressibility factor
- V = volume
- B = second virial coefficient
- C = third virial coefficient
- etc....

A similar expansion of Z as power series in P has nevertheless found considerable use,

$$Z = 1 + B^1 P + C^1 P^2 + D^1 P^3 + \dots \quad (6)$$

where $B^1, C^1, D^1 \dots$ are constants

and $Z = \frac{PV}{RT}$

then, $V = \frac{ZRT}{P} \dots \quad (7)$

By substituting the value of V from equation (7) into equation (5) then,

$$\frac{Z-1}{P} = \frac{B}{ZRT} + \frac{CP}{(ZRT)^2} + \frac{DP^2}{(ZRT)^3} + \dots \quad (8)$$

Differentiating equation (8) with respect to pressure at constant temperature gives,

$$\left[\frac{\partial \left(\frac{Z-1}{P} \right)}{\partial P} \right]_T = - \frac{B}{Z^2 RT} \left(\frac{\partial Z}{\partial P} \right) + \frac{C}{(ZRT)^2} \left[1 - \frac{2P}{Z} \left(\frac{\partial Z}{\partial P} \right) \right]$$

$$+ \frac{DP}{(ZRT)^3} \left[2 - \frac{3P}{Z} \left(\frac{\partial Z}{\partial P} \right) \right] + \dots \dots \dots (9)$$

As pressure approaches zero, equation (9) becomes,

$$\lim_{P \rightarrow 0} \left(\frac{Z-1}{P} \right) = \frac{B}{RT} \dots \dots \dots (10)$$

If the expansion for Z is written directly in P, that is, equation (6)

$$\lim_{P \rightarrow 0} \frac{Z-1}{P} = B^1 \dots \dots \dots (11)$$

Application of L'Hospital rule shows this limit also to be

$$\left(\frac{\partial Z}{\partial P} \right)_T$$

Then we have,

$$B^1 = \frac{B}{RT} = \lim_{P \rightarrow 0} \left(\frac{\partial Z}{\partial P} \right)_T \dots \dots \dots (12)$$

By taking the limit of equation (9),

$$\begin{aligned} \lim_{P \rightarrow 0} \left[\frac{\partial \left(\frac{Z-1}{P} \right)}{\partial P} \right]_T &= - \frac{B^2}{(RT)^2} + \frac{C}{(RT)^2} \\ &= \frac{C - B^2}{(RT)^2} \dots \dots \dots (13) \end{aligned}$$

But from equation (6)

$$\left[\frac{\partial \left(\frac{Z-1}{P} \right)}{\partial P} \right]_T = C^1 + 2D^1 P + \dots \dots \dots$$

$$\lim_{P \rightarrow 0} \frac{\partial \left(\frac{Z-1}{P} \right)}{\partial P} = C^1 \dots \dots \dots (14)$$

By comparing equations (14) and (13), it gives,

$$C^1 = \frac{C - B^2}{(RT)^2} \dots \dots \dots (15)$$

We may now write equation (6), by substituting the values of B^1 , C^1, as follows,

$$Z = 1 + \frac{B}{RT} P + \frac{C-B^2}{(RT)^2} P^2 + \dots \dots \dots (16)$$

Since, $\ln \phi = - \frac{1}{RT} \int_0^P a \, dP \dots \dots \dots (17)$

where, $a = \text{Residual volume}$
 $= \left(\frac{RT}{P} - V \right)$

by rearrangement,

$$\begin{aligned} a &= \frac{RT}{P} \left(1 - \frac{Pv}{RT} \right) \\ &= \frac{RT}{P} (1 - Z) \dots \dots \dots (18) \end{aligned}$$

Substitute the value of a from equation (18) into equation (17), we get,

$$\ln \phi = \int_0^P (Z - 1) \frac{dP}{P} \quad (\text{at constant temperature}) \dots \dots \dots (19)$$

The most convenient substitution for (Z - 1) is by equation (16) truncated to three terms:

$$\ln \eta = \int_0^P \left[\frac{B}{RT} + \frac{C - B^2}{(RT)^2} P \right] dP$$

integration gives,

$$\ln \eta = \frac{BP}{RT} + \left(\frac{C - B^2}{2} \right) \left(\frac{P}{RT} \right)^2 \dots \dots \dots (20)$$

At low pressures a further approximation may be made by truncating the virial equation (20) to just one term, i.e.

$$\ln \eta = \frac{BP}{RT} \dots \dots \dots (21)$$

Then for the component i, equation (21) will be,

$$\ln \eta_i = \frac{B_{ii} P}{RT} \dots \dots \dots (22)$$

where,

B_{ii} = second virial coefficient of the pure component i.

Secondly, for η_i^L

At temperature T and the vapor pressure of pure component i, the fugacity coefficient for the liquid phase is equal to the fugacity coefficient of the vapor phase and is therefore represented by the same equation

$$\ln \eta_i^L = \frac{B_{ii} p^i}{RT}$$

where the (') indicates the values at the vapor pressure.

Now the change in $\ln \phi_i^L$ in going from the vapor pressure p_i' to the pressure P is given by integration of equation (17)

$$\begin{aligned} \ln \phi_i^L - \ln \phi_i' &= \int_{p_i'}^P - \frac{a_i}{RT} dP \\ &= \frac{1}{RT} \int_{p_i'}^P \left(V_i^L - \frac{RT}{P} \right) dP \dots\dots\dots (24) \end{aligned}$$

Since the change of a liquid's volume with pressure is very small, V_i^L may be considered as a constant. Then by integration, we get,

$$\ln \phi_i^L = \frac{B_{ii} p_i'}{RT} + \frac{V_i^L}{RT} (P - p_i') - \ln \frac{P}{p_i'} \dots\dots\dots (25)$$

Thirdly, for γ_i^V

From equation (21)

$$\ln \phi = \frac{BP}{RT}$$

Similarly for pure i

$$\ln \phi_i = \frac{B_{ii} P}{RT} \dots\dots\dots (26)$$

For binary system B is given by,

$$B = y_1 B_{11} + y_2 B_{22} + y_1 y_2 \delta_{12} \dots\dots\dots (27)$$

where

B = second virial coefficient of the mixture

B_{11} = second virial coefficient of pure component 1

B_{22} = second virial coefficient of pure component 2

y_1, y_2 = mole fraction of component 1 and 2 in the vapor phase respectively

δ_{12} = cross coefficient of component 1 and 2

The fugacity coefficient can be written in terms of the mole fraction of the gas phase

$$\ln \hat{\phi}_j = \ln \phi + \frac{\partial \ln \phi}{\partial y_j} - \sum_i \left(y_i \frac{\partial \ln \phi}{\partial y_i} \right) \dots \dots \dots (28)$$

where,

$\hat{\phi}_j$ = fugacity coefficient of the component j in solution

ϕ = fugacity coefficient of the mixture

for binary system,

$$\ln \hat{\phi}_1 = \ln \phi + \frac{\partial \ln \phi}{\partial y_1} - y_1 \frac{\partial \ln \phi}{\partial y_1} - y_2 \frac{\partial \ln \phi}{\partial y_2}$$

$$\text{or } \ln \hat{\phi}_1 = \ln \phi + (1-y_1) \frac{\partial \ln \phi}{\partial y_1} - y_2 \frac{\partial \ln \phi}{\partial y_2}$$

$$\text{or } \ln \hat{\phi}_1 = \ln \phi + y_2 \left(\frac{\partial \ln \phi}{\partial y_1} - \frac{\partial \ln \phi}{\partial y_2} \right) \dots \dots \dots (29)$$

From equation (21), and (27),

$$\frac{\partial \ln \phi}{\partial y_1} = \frac{P}{RT} \frac{\partial B}{\partial y_1} = \frac{P}{RT} (B_{11} + y_2 \delta_{12}) \dots\dots\dots (30)$$

$$\text{and, } \frac{\partial \ln \phi}{\partial y_2} = \frac{P}{RT} \frac{\partial B}{\partial y_2} = \frac{P}{RT} (B_{22} + y_1 \delta_{12}) \dots\dots\dots (31)$$

By substituting the values of (30) and (31) into equation (29), we get,

$$\begin{aligned} \ln \hat{\phi}_1 &= \frac{PB}{RT} + \frac{Py_2}{RT} (B_{11} + y_2 \delta_{12} - B_{22} - y_1 \delta_{12}) \\ &= \frac{P}{RT} B + B_{11} - y_1 B_{11} + y_2 B_{22} + y_1 y_2 \delta_{12} + y_2^2 \delta_{12} \end{aligned}$$

$$\text{but } B = y_1 B_{11} + y_2 B_{22} + y_1 y_2 \delta_{12}$$

$$\ln \hat{\phi}_1 = \frac{P}{RT} (B_{11} + y_2^2 \delta_{12}) \dots\dots\dots (32)$$

Similarly in the same way,

$$\ln \hat{\phi}_2 = \frac{P}{RT} (B_{22} + y_1^2 \delta_{12}) \dots\dots\dots (33)$$

By definition the fugacity coefficient of component i in solution is given by,

$$\hat{\phi}_i = \frac{\hat{f}_i}{\kappa_i P} \dots\dots\dots (34)$$

where,

\hat{f}_i = fugacity of component i in solution

x_i = mole fraction of component i in liquid phase

P = pressure of the system

and, for pure component,

$$\phi_i = \frac{\hat{f}_i}{P} \dots\dots\dots (35)$$

where,

f_i° = fugacity of the pure component i

Then,

$$\gamma_i = \frac{\hat{f}_i}{x_i f_i^\circ} = \frac{\hat{f}_i / P \phi_i}{f_i^\circ / P} = \frac{\phi_i}{\phi_i^\circ} \dots\dots\dots (36)$$

where,

f_i° = fugacity of the pure component i in some convenient standard state

γ_i = activity coefficient

Then,

$$\ln \gamma_i = \ln \phi_i - \ln \phi_i^\circ \dots\dots\dots (37)$$

From equation (21), and (32),

$$\ln \gamma_1 = \frac{P}{RT} (B_{11} + \gamma_2^2 \delta_{12} - B_{11})$$

Then,

$$\ln y_1 = \frac{P}{RT} y_2^2 \delta_{12} \dots\dots\dots (38)$$

and, similarly in the same way,

$$\ln y_2 = \frac{P}{RT} y_1^2 \delta_{12} \dots\dots\dots (39)$$

In equation (4), we substitute the values of ϕ_i^V , ϕ_i^L , y_i^V given by equation (22) and (37) respectively we get,

$$\ln y_1^L = \frac{\ln y_1 P}{x_1 P_1} + \frac{(B_{11} - V_1^L)(P - P_1)}{RT} + \ln y_1^V \dots\dots\dots (40)$$

For binary system,

$$\ln y_1^L = \frac{\ln y_1 P}{x_1 P_1} + \frac{(B_{11} - V_1^L)(P - P_1)}{RT} + \frac{P \delta_{12} y_2^2}{RT} \dots\dots (41)$$

and,

$$\ln y_2^L = \frac{\ln y_2 P}{x_2 P_2} + \frac{(B_{22} - V_2^L)(P - P_2)}{RT} + \frac{P \delta_{12} y_1^2}{RT} \dots\dots (42)$$

where,

$$\delta_{12} = B_{12} - B_{11} - B_{22}$$

and, B_{12} is the cross coefficient.

The value of the second virial coefficients of the pure components, B_{11} and B_{22} can be calculated if the critical properties of the components are known. These may be calculated by the correlation given by Pitzer and Curl ⁽³⁰⁾.

The value of the cross coefficient can be evaluated using the correlation proposed by O'Connell and Prausnitz ⁽³¹⁾.

Correlation of Data

A number of integrated forms of the Gibbs-Duhem equation are available for correlating activity coefficients. They are:

1. Redlich-Kister equations
2. Margule's equation ⁽⁴⁾
3. Van Laar equation ⁽⁵⁾
4. Scatchard-Hamer equation
5. Norrish-Twigg equation
6. Prahl equation
7. Gilman equation
8. Method of Hirati

The most important is:

Redlich-Kister equations: ⁽¹⁾

These are the most commonly used for correlating the liquid activity coefficients with the liquid phase composition.

The authors started from the molar excess free energy, especially the "Q function", which is related to the molar excess free energy by the following simple relation,

$$Q = \frac{\Delta G^E}{2.303 RT}$$

for a binary system,

$$Q = x_1 \log \gamma_1 + x_2 \log \gamma_2 \dots\dots\dots (43)$$

where,

x_1, x_2 = mole fraction of the component 1 and 2, in the liquid phase respectively

γ_1, γ_2 = activity coefficient of the component 1 and 2 in the liquid phase respectively

The usual convention,

$$\gamma_1 = 1 \quad \text{at } x_1 = 1$$

$$\gamma_2 = 1 \quad \text{at } x_2 = 1$$

is adopted.

The function Q will be equal to zero for a perfect solution at any concentration. It is also zero for any solution at the end points $x_1 = 1$ and $x_2 = 1$. Redlich and Kister⁽¹⁾ proposed that the Q function can be represented by an appropriate power series of the liquid composition.

The expansion for a binary system is given by,

$$Q = x_1 x_2 \left[B_{12} + C_{12} (x_1 - x_2) + D_{12} (x_1 - x_2)^2 \right] \dots \quad \text{at } (T, P)$$

where the constants $B_{12}, C_{12}, D_{12}, \dots$ depend on temperature only.

Differentiating equation (43) with respect to x_1 we get,

$$\frac{dQ}{dx_1} = \log \gamma_1 / \gamma_2 \dots\dots\dots (44)$$

and the individual activity coefficients are

$$\log \gamma_1 = Q + x_2 \frac{dQ}{dx_1} \dots\dots\dots (45)$$

$$\log \gamma_2 = Q - x_1 \frac{dQ}{dx_2} \dots\dots\dots (46)$$

so that,

$$\log \gamma_1 = x_2^2 \left[B_{12} + C_{12} (3x_1 - x_2) + D_{12} (x_1 - x_2)(5x_1 - x_2) \right. \\ \left. + \dots\dots\dots \right] \dots\dots\dots (47)$$

and,

$$\log \gamma_2 = x_1^2 \left[B_{12} + C_{12} (x_1 - 3x_2) + D_{12} (x_1 - x_2)(x_1 - 5x_2) \right. \\ \left. + \dots\dots\dots \right] \dots\dots\dots (48)$$

The function,

$$\frac{dQ}{dx} = \log \gamma_1 / \gamma_2$$

is suitable for the following reasons,

- (a) The function Q, given by (44), is the simple relationship between the experimental data and, the technically important,

$$\frac{dQ}{dx_1} = \log \gamma_1 / \gamma_2 \dots\dots\dots (44)$$

and the individual activity coefficients are

$$\log \gamma_1 = Q + x_2 \frac{dQ}{dx_1} \dots\dots\dots (45)$$

$$\log \gamma_2 = Q - x_1 \frac{dQ}{dx_2} \dots\dots\dots (46)$$

so that,

$$\log \gamma_1 = x_2^2 \left[B_{12} + C_{12} (3x_1 - x_2) + D_{12} (x_1 - x_2)(5x_1 - x_2) \right. \\ \left. + \dots\dots\dots \right] \dots\dots\dots (47)$$

and,

$$\log \gamma_2 = x_1^2 \left[B_{12} + C_{12} (x_1 - 3x_2) + D_{12} (x_1 - x_2)(x_1 - 5x_2) \right. \\ \left. + \dots\dots\dots \right] \dots\dots\dots (48)$$

The function,

$$\frac{dQ}{dx} = \log \gamma_1 / \gamma_2$$

is suitable for the following reasons,

- (a) The function Q, given by (44), is the simple relationship between the experimental data and, the technically important,

relative volatility,

$$\alpha = \frac{y(1-x)}{x(1-y)}$$

$$\log \alpha = \log \gamma_1 / \gamma_2 + \log (P_1^\circ / P_2^\circ) \dots\dots\dots (49)$$

where,

y = mole fraction in the vapor

x = mole fraction in the liquid

γ_1, γ_2 = activity coefficient of component 1 and 2 in the liquid phase

P_1°, P_2° = vapor pressure of pure components 1 and 2 at temperature of system

the vapor phase is assumed to be perfect.

(b) The function $\log \gamma_1 / \gamma_2$ provides an efficient tool for eliminating inconsistencies in the experimental data. Since Ω according to equation (43), has the values zero for $x = 0$ and $x = 1$, then

$$\int_0^1 \log (\gamma_1 / \gamma_2) dx = 0 \dots\dots\dots (50)$$

If the $\log \gamma_1 / \gamma_2$ is plotted against x_1 , from $x_1 = 0$ to $x_1 = 1$, the net area under the curve should be equal to zero.

The area condition applies only at constant temperature.

It should be mentioned that Redlich-Kister equation does not

relative volatility,

$$a = \frac{y(1-x)}{x(1-y)}$$

$$\log a = \log \gamma_1 / \gamma_2 + \log (p^*_1 / p^*_2) \dots\dots\dots (49)$$

where,

y = mole fraction in the vapor

x = mole fraction in the liquid

γ_1, γ_2 = activity coefficient of component 1 and 2 in the liquid phase

p^*_1, p^*_2 = vapor pressure of pure components 1 and 2 at temperature of system

the vapor phase is assumed to be perfect.

(b) The function $\log \gamma_1 / \gamma_2$ provides an efficient tool for eliminating inconsistencies in the experimental data. Since Q according to equation (43), has the values zero for $x = 0$ and $x = 1$, then

$$\int_0^1 \log (\gamma_1 / \gamma_2) dx = 0 \dots\dots\dots (50)$$

If the $\log \gamma_1 / \gamma_2$ is plotted against x_1 , from $x_1 = 0$ to $x_1 = 1$, the net area under the curve should be equal to zero.

The area condition applies only at constant temperature.

It should be mentioned that Redlich-Kister equation does not

have to be limited to the three constants as shown in the equation (47) and (48).

In general, the series furnishes for each case the most convenient representation ⁽¹⁾. According to Redlich, Kister and Turnquist ⁽¹²⁾ only the first term is required for nearly perfect solutions.

For solution containing an associated component, such as alcohols and acids, the third term is necessary. However, only very accurate measurements for extremely imperfect solutions require four terms.

This is further reported by Lu ⁽³²⁾, that three constant Redlich-Kister equations are adequate for representing liquid activity coefficients for most of the systems.

CHAPTER IV

EXPERIMENTAL DETAILS

I. (1) Materials

Spectroquality benzene of Matheson Coleman and Bell, and n-octane (99.9 mole % minimum) supplied by Phillips petroleum Company, were used. Physical properties of the chemicals are listed in Table 1.

TABLE I

Material	N. B. pt °C		Ref. index at 25° C	
	Expt.	Lit (33)	Expt.	Lit (33)
Benzene	80.10	80.103	1.4979	1.4979
n-octane	125.62	125.662	1.39513	1.39505

(2) Apparatus

(a) Equilibrium still:

The equilibrium still used in this work is illustrated in Figure (1). It is a circulating still of the Gillespie type, modified by Fowler and Norris⁽³⁴⁾. They modified the original Gillespie still by the addition of a liquid receiver.

The liquid separated in the equilibrium chamber flows to the liquid receiver and returns to the boiling flask. A sample withdrawn from the liquid receiver represents the liquid which is in

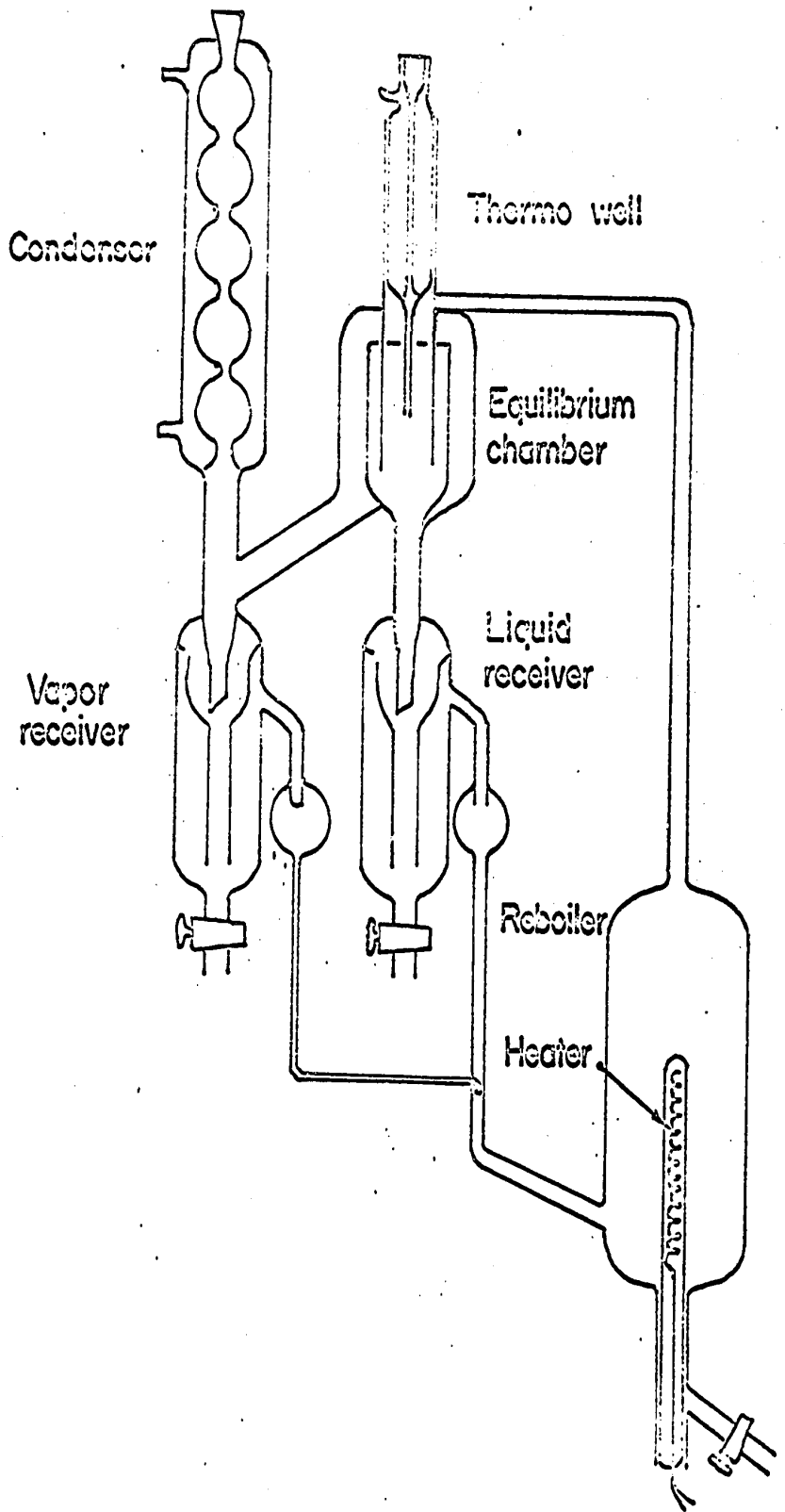


Figure 1. Schematic diagram of the modified Gillespie :
equilibrium still

- A To vacuum pump
- B 3-way joint
- C Cold trap
- D To vapor condenser
- E Mercury manometer
- F 3-way joint
- G Surge tank
- H Cartesian manostat
- V To vent

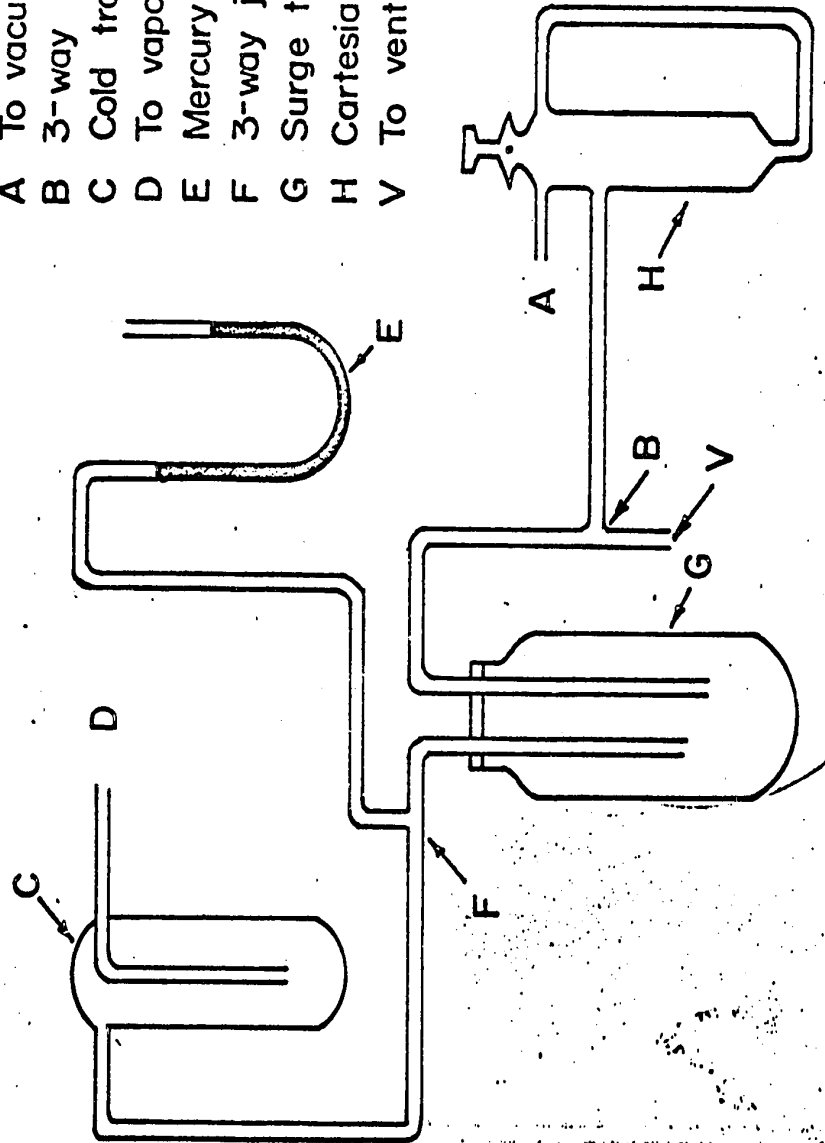


Figure 2. Sketch of the pressure control system

equilibrium with the vapor phase condensed in the vapor receiver.

The present still differs from the modified one in the following ways:

- (1) To obtain better measurement of the temperature, a vacuum sealed double jacketed glass thermowell was used for the insertion of the hot junction of the thermocouple.
- (2) To obtain better mixing in the liquid and vapor receiver, a double jacket was used instead of the simple tubing.
- (3) To avoid air bubble formation where the heater was inserted, and also eliminate any possible leakage, the internal heater was sealed at the bottom of the boiler, instead of being inserted at the top.
- (4) To eliminate any possible contamination by stop-cock grease, Teflon stop-cocks were used instead of glass ones.

The still was made of pyrex glass. The boiler was heated by the internal heater which was controlled by a powerstat.

The Cottrell pump and the equilibrium chamber were insulated with 0.5 inch layer of asbestos.

(b) Accessory equipment used with the still

They are divided into two parts,

- (i) Temperature measurement devices
- (ii) Pressure measurement devices

(i) Temperature measurement devices

Temperature was measured by means of an iron-constantan thermocouple. The thermocouple was calibrated by comparison with a standard platinum resistance thermometer. The uncertainty of the calibration was 0.02° C.

The calibration curve shown in Figure (15) and listed in Table 3.

When the still was in operation, the hot junction was placed in a thermowell of the still. A few drops of silicone 704 Dow-corning silicone was added at this junction to provide good contact. The cold junction was immersed in an ice-water bath in a Dewar flask. The corresponding e.m.f. was measured by means of Leeds and Northrup K-3 potentiometer with SRI Tensley galvanometer.

For isothermal operation, the desired temperatures 75° C, 65° C, and 55° C, were obtained, and regulated by adjusting the total pressure of the system. A diagram of the pressure control system which consists of a cold trap, a surge tank, and a cartesian monostat connected in series is shown in Figure 2.

(ii) Pressure measurement device

The pressure of the system was read from a mercury manometer.

(c) Equipment for quantitative analysis

Refractometer

A Bausch and Lomb Abb-3L precision refractometer and sodium lamp were used to determine the refractive indices of the mixtures.

The prism temperature was kept constant at $25^{\circ}\text{C} \pm 0.02^{\circ}\text{C}$. The calibration curve was obtained by measuring the refractive indices of mixtures of known composition.

The known composition of the mixtures were determined analytically by weighing the components individually using an

analytical balance. The calibration values are shown in Table (4) and Figure (16).

II. Experimental Procedure

1. Test of the equilibrium still

The equilibrium still was used previously to obtain γ -x-P-T data on the following systems:

- (i) Ethanol water at 760 mm Hg ⁽³⁵⁾, the data obtained was in agreement with those of Otuski and Williams ⁽³⁶⁾.
- (ii) Benzene-n-heptane at 80° C and 760 mm Hg ⁽³⁷⁾, the results obtained agreed with those reported by Brown ⁽³⁸⁾ and Myers ⁽³⁹⁾.
- (iii) Before this study, a series of runs were performed on the system Benzene-n-heptane at 75° C, the results were in complete agreement with those of Lu ⁽⁴⁰⁾.

2. Binary system of Benzene-n-octane

(a) Preparation of the binary liquid mixture

The still was filled with the less volatile component first. The boiling point of the pure components were determined. Then mixtures of increasing amount of the more volatile were added for the successive runs.

(b) Procedure

The reboiler, the liquid receiver, and the vapor condensate receiver were filled with the mixture at the beginning of each run.

The heater in the reboiler should always be fully immersed into the liquid.

The temperature in the still was controlled at $\pm 0.1^\circ\text{C}$

of the desired temperature by adjusting the total pressure of the still. The still was allowed to operate 4-5 hours to ensure attainment of equilibrium.

Barometric pressure, system pressure, and temperature of the system were recorded before samples were withdrawn for analysis. Before sampling, several milliliters of samples were taken to flush the lines.

Sample bottles were cool enough to prevent any evaporation during sampling.

CHAPTER V

RESULTS

Data for the binary system benzene-n-octane at the three isothermal conditions 75° C, 65° C, and 55° C are given in Table (2) and Figures (3)(4). . . . (14).

TABLE (2)

VAPOUR-LIQUID EQUILIBRIUM DATA

Temp. °C	Pressure mm. Hg	x_B	y_B	Y_B	Y_O	z'_B	z'_O	
75.0	628.4	0.9570	0.9850	0.999	1.464	1.001	0.955	
	595.6	0.8820	0.9590	1.002	1.374	1.003	0.958	
	5.449	0.7350	0.9130	1.049	1.190	1.005	0.963	
	530.9	0.7210	0.9091	1.038	1.152	1.006	0.964	
	502.7	0.6505	0.8550	1.062	1.104	1.067	0.966	
	485.2	0.6091	0.8680	1.075	1.095	1.008	0.968	
	466.9	0.5690	0.8540	1.091	1.059	1.008	0.970	
	419.5	0.4730	0.8030	1.111	1.054	1.011	0.974	
	412.7	0.4512	0.7901	1.128	1.062	1.012	0.974	
	399.8	0.4330	0.7822	1.128	1.035	1.012	0.976	
	361.9	0.3650	0.7305	1.133	1.038	1.014	0.979	
	333.8	0.3150	0.6970	1.157	1.000	1.016	0.982	
	277.4	0.2051	0.5710	1.214	1.020	1.018	0.987	
	65.0	450.5	0.9541	0.9859	1.000	1.348	1.001	0.964
		440.1	0.9152	0.9741	1.006	1.342	1.001	0.966
		434.6	0.8940	0.9679	1.011	1.313	1.002	0.966
414.5		0.8250	0.9470	1.023	1.252	1.003	0.968	
409.9		0.7890	0.9343	1.037	1.266	1.003	0.968	
397.2		0.7663	0.9248	1.033	1.278	1.004	0.969	
396.8		0.7472	0.9214	1.054	1.232	1.004	0.969	
383.9		0.7150	0.9142	1.055	1.155	1.004	0.970	
380.3		0.7085	0.9108	1.054	1.163	1.005	0.971	
368.9		0.6730	0.8990	1.063	1.144	1.005	0.972	
361.8		0.6519	0.8960	1.066	1.142	1.005	0.973	
348.6		0.6112	0.8812	1.085	1.068	1.006	0.974	
337.0		0.5630	0.8660	1.110	1.075	1.007	0.975	

TABLE (2) continued

Temp. °C	Pressure mm. Hg	x_B	y_B	Y_B	Y_O	x'_B	x'_O
	336.5	0.5520	0.8550	1.126	1.094	1.007	0.975
	329.1	0.5550	0.8580	1.100	1.055	1.007	0.976
	321.7	0.5301	0.8300	1.106	1.151	1.008	0.977
	311.6	0.5042	0.8353	1.117	1.042	1.008	0.978
	301.0	0.4703	0.8187	1.134	1.038	1.009	0.979
	289.0	0.4400	0.8030	1.142	1.026	1.010	0.980
	282.7	0.4231	0.7991	1.157	1.042	1.010	0.981
	277.4	0.4140	0.7881	1.149	1.013	1.010	0.981
	251.6	0.3480	0.7466	1.171	1.009	1.012	0.984
	230.9	0.3062	0.7015	1.149	1.008	1.013	0.985
	227.9	0.2951	0.6960	1.168	1.021	1.013	0.986
	223.3	0.2820	0.6816	1.173	1.021	1.013	0.987
	193.5	0.2110	0.5910	1.180	1.022	1.014	0.990
55.1	310.2	0.9176	0.9691	1.002	1.930	1.001	0.972
55.0	295.4	0.8276	0.9491	1.027	1.350	1.002	0.974
	292.5	0.8275	0.9462	1.024	1.417	1.002	0.974
	290.5	0.8184	0.9440	1.026	1.387	1.002	0.974
	286.7	0.8042	0.9440	1.031	1.265	1.002	0.975
	284.0	0.7930	0.9383	1.030	1.309	1.003	0.976
	283.1	0.7803	0.9348	1.039	1.298	1.003	0.975
	279.4	0.7700	0.9316	1.036	1.287	1.003	0.976
	276.6	0.7470	0.9280	1.053	1.214	1.003	0.976
	275.5	0.7601	0.9321	1.034	1.205	1.003	0.976
	274.0	0.7389	0.9259	1.053	1.202	1.003	0.976
	267.5	0.7220	0.9199	1.044	1.202	1.003	0.977
	264.8	0.6940	0.9150	1.071	1.376	1.004	0.977
	259.8	0.6721	0.9061	1.075	1.151	1.004	0.978
	252.3	0.6536	0.9013	1.068	1.113	1.004	0.979
	252.1	0.6421	0.8925	1.075	1.172	1.004	0.979
	241.3	0.5891	0.8781	1.111	1.109	1.005	0.980
	230.4	0.5535	0.8650	1.111	1.080	1.006	0.981
	227.5	0.5392	0.8594	1.114	1.077	1.006	0.981
	226.8	0.5336	0.8550	1.117	1.077	1.006	0.981
	218.7	0.5105	0.8471	1.116	1.062	1.006	0.982
	205.1	0.4450	0.8209	1.165	1.031	1.007	0.984
	199.1	0.4260	0.8093	1.165	1.050	1.007	0.984

TABLE (2) continued

Temp. °C	Pressure mm. Hg	x_B	y_B	γ_B	γ_O	z'_B	z'_O
181.2		0.3630	0.7530	1.159	1.098	1.008	0.986
171.8		0.3339	0.7470	1.186	1.019	1.009	0.988
156.0		0.2811	0.7020	1.204	1.012	1.010	0.990
143.4		0.2589	0.6676	1.142	1.008	1.011	0.990
126.6		0.1833	0.5783	1.235	1.026	1.012	0.992

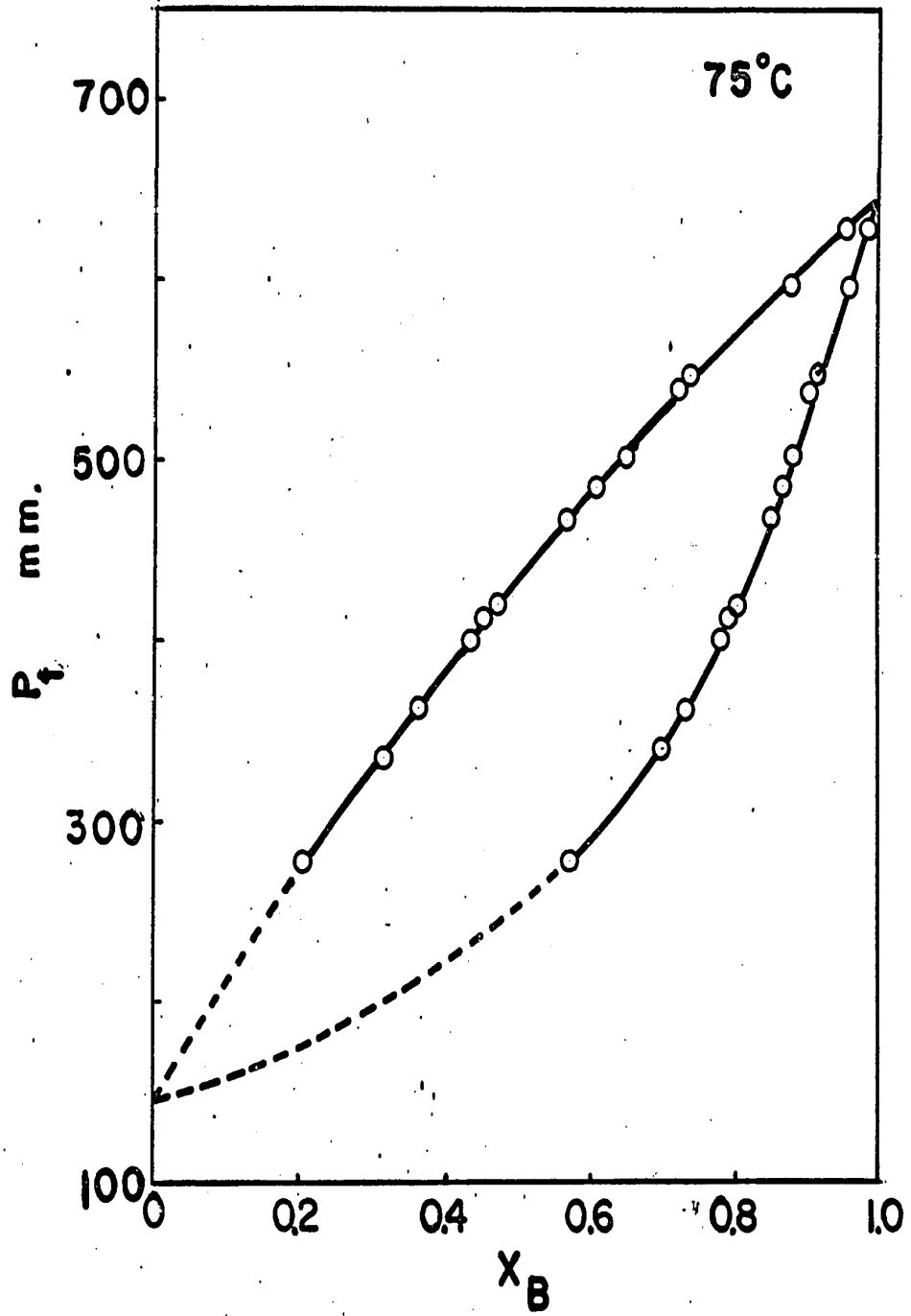


FIGURE 3: Total pressure - composition diagram for the system benzene (B) - n-octane(O) at 75°C.

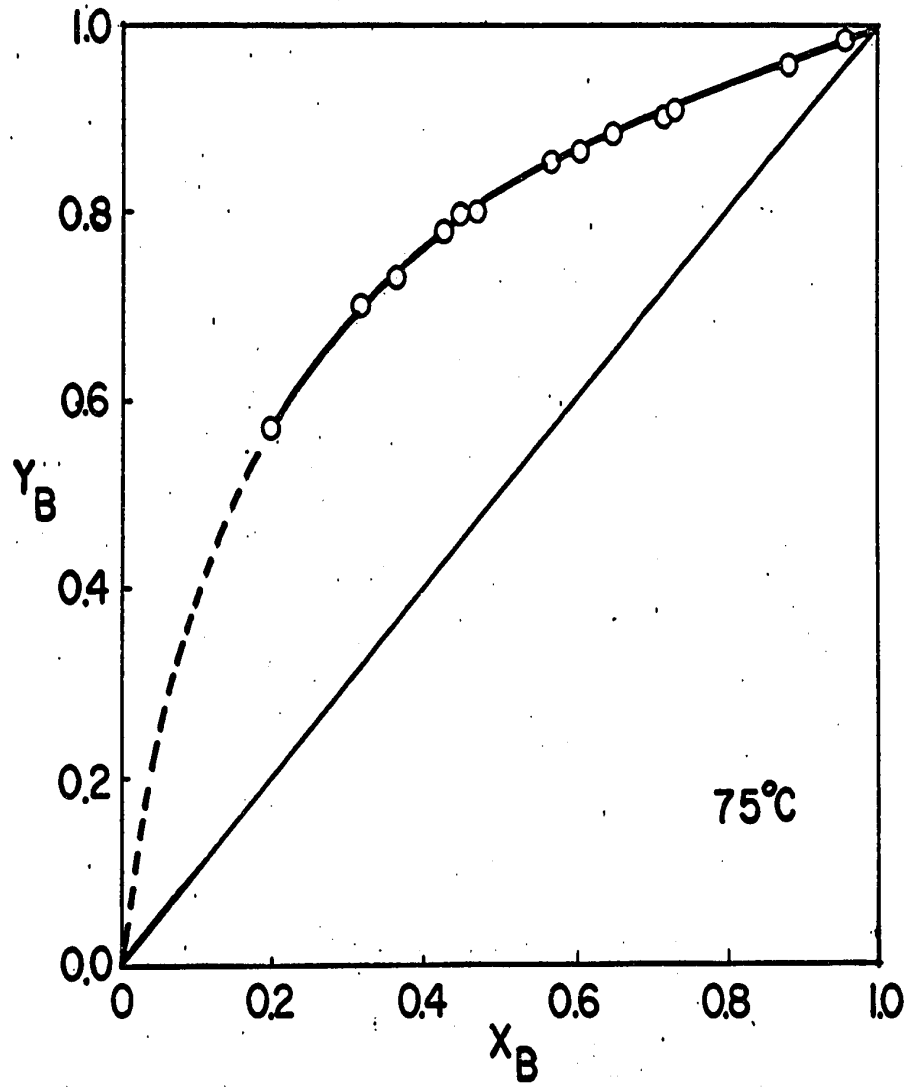


FIGURE 4: x - y curve for the system benzene (B) - n-octane (O) at 75° C.

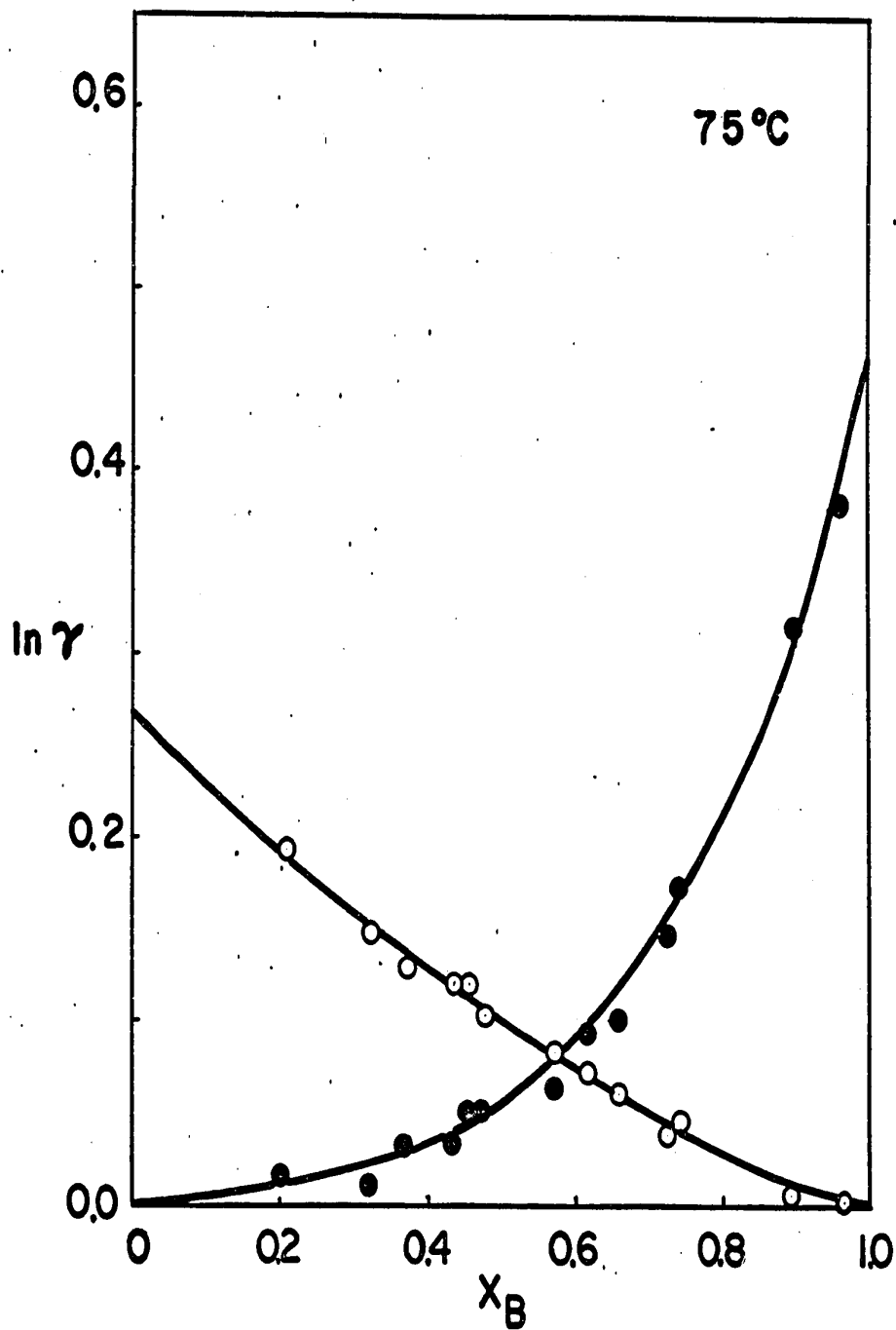


FIGURE 5: Liquid activity coefficient - composition, for the system benzene (B) -n-octane (O) at 75° C.

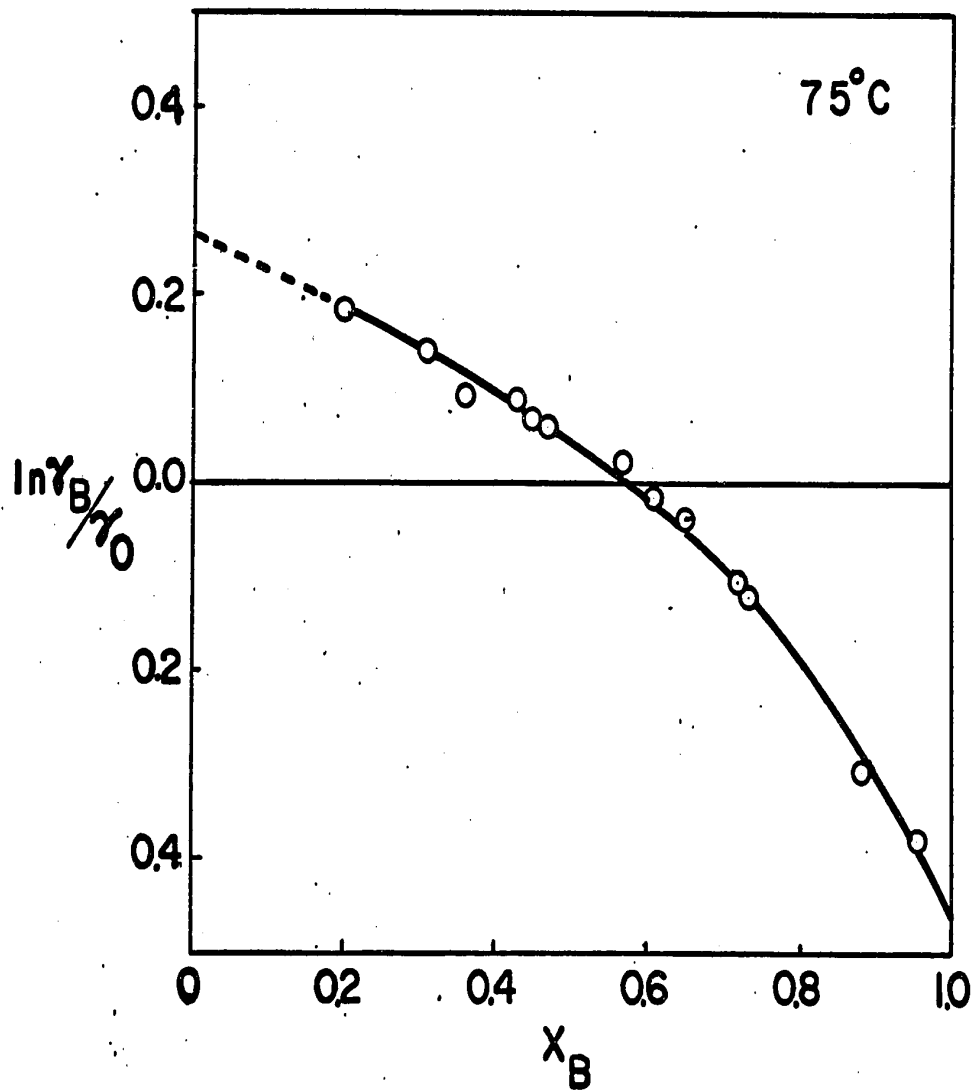


FIGURE 6: $\ln \gamma_B / \gamma_0$ - composition for the system benzene
(B) -n-octane (O) at 75°C.

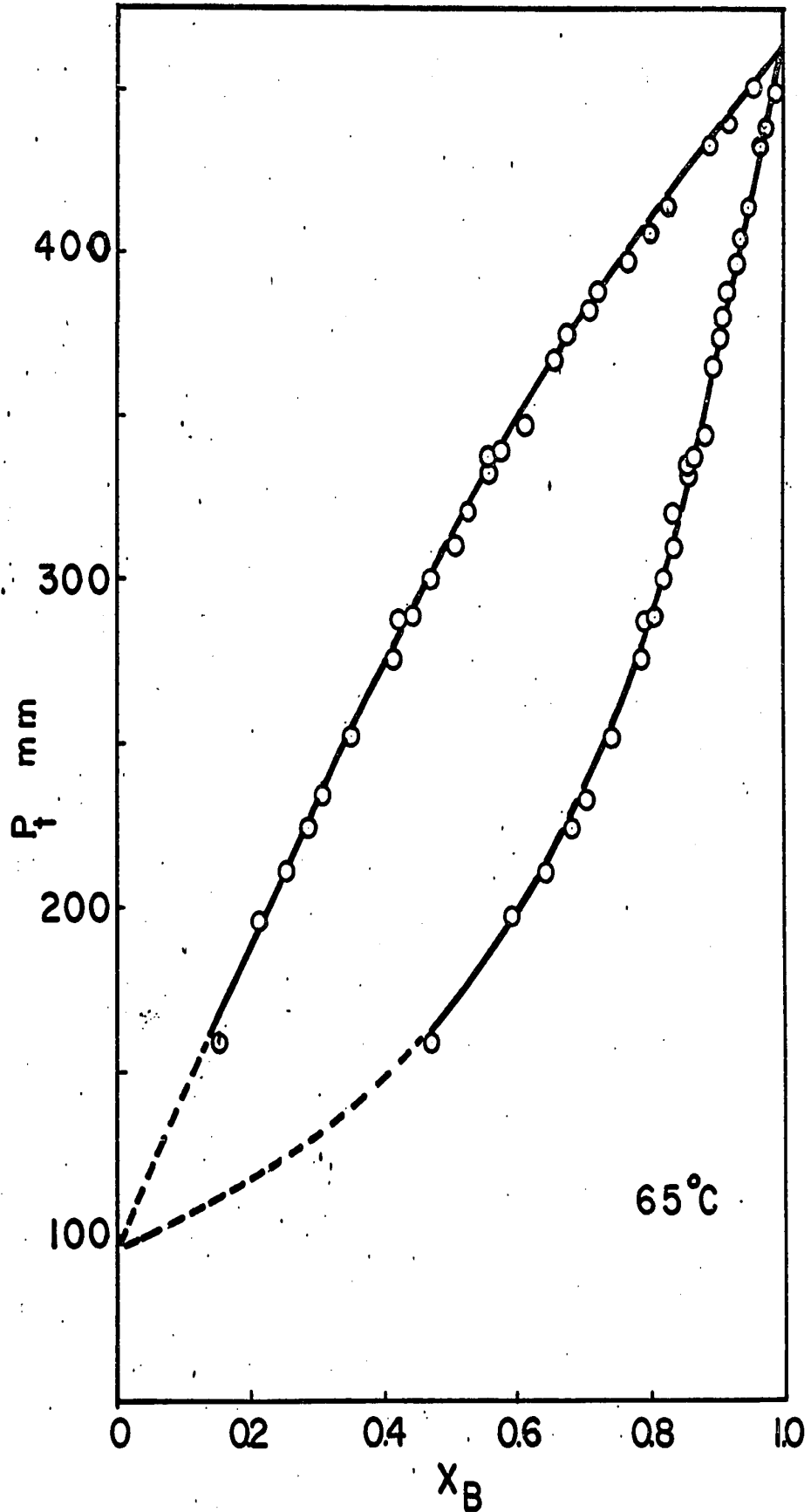


FIGURE 7: Total pressure - composition diagram for the system benzene (B) - n-octane (O) at 65°C .

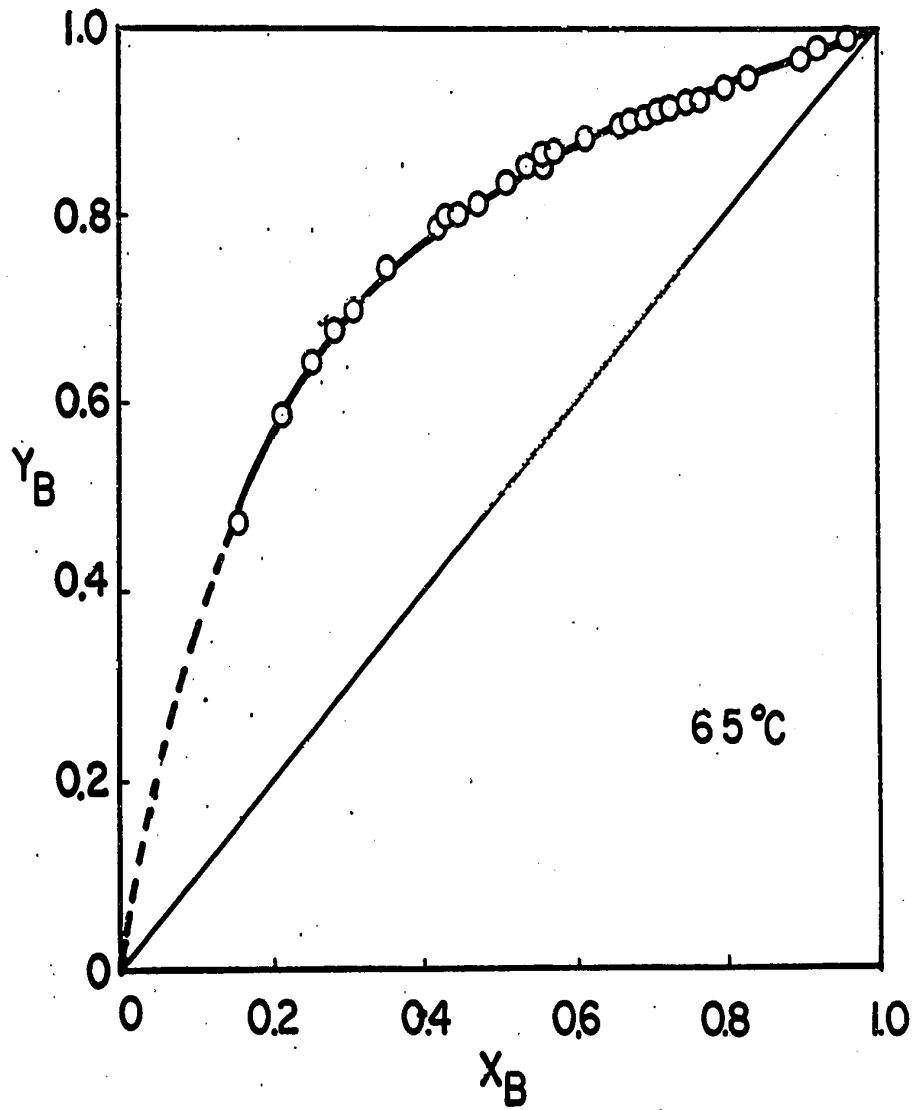


FIGURE 8: x - y curve for the system benzene (B) - n-octane (O) at 65°C.

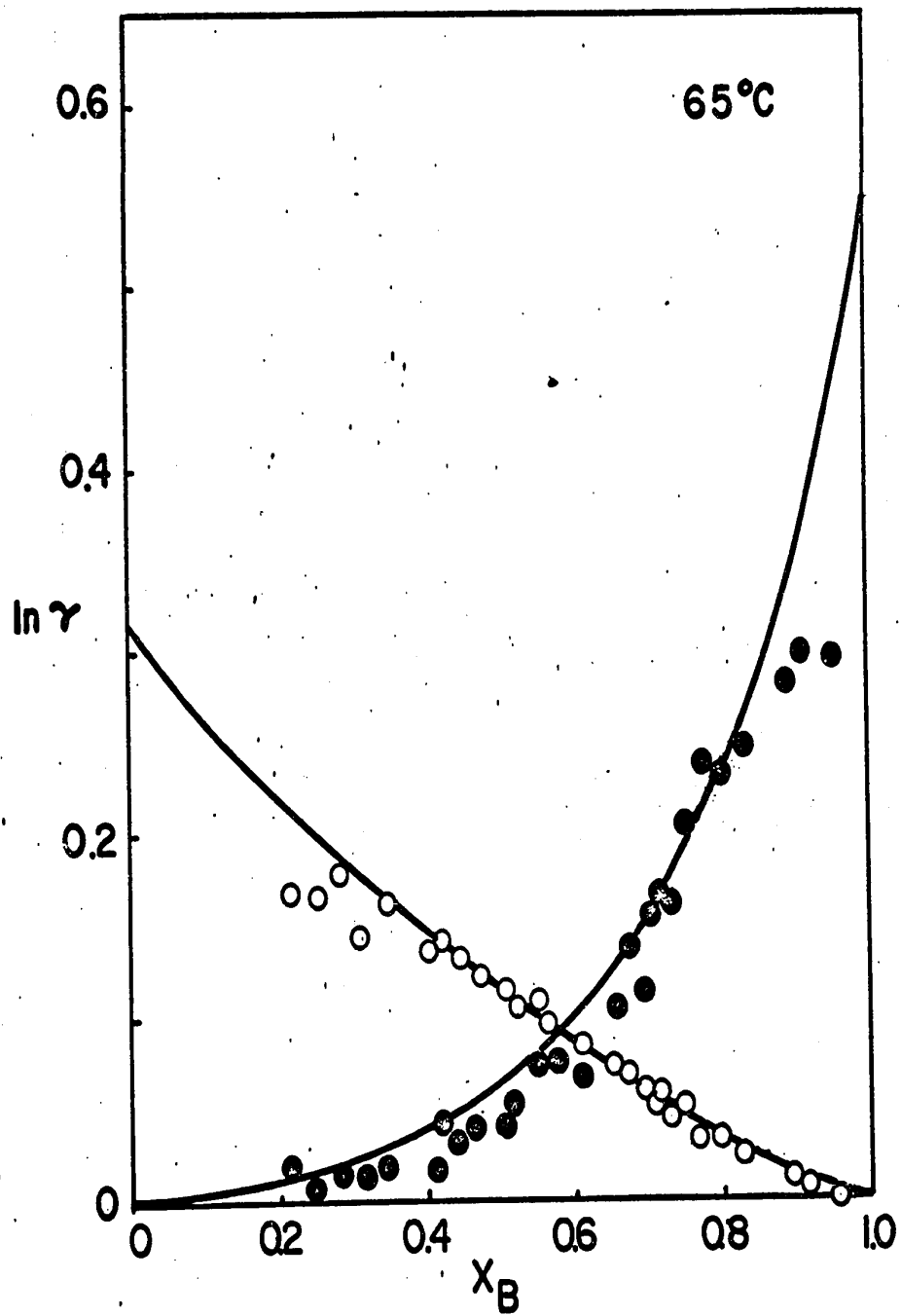


FIGURE 9: Activity coefficient vs. composition for benzene (B) -n-octane at 65° C.

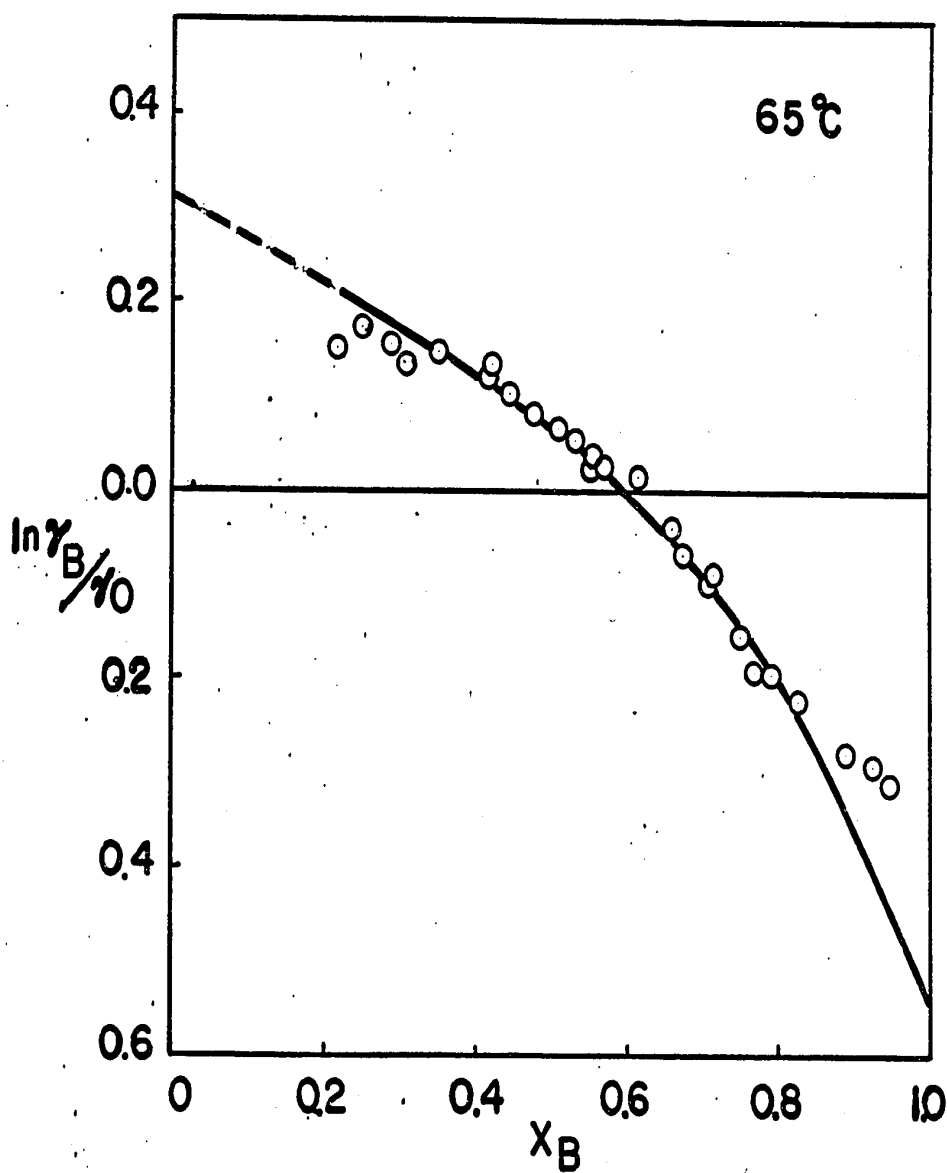


FIGURE 10: $\ln \gamma_B/\gamma_0$ - composition for the system benzene
(B) -n-octane (O) at 65°C .

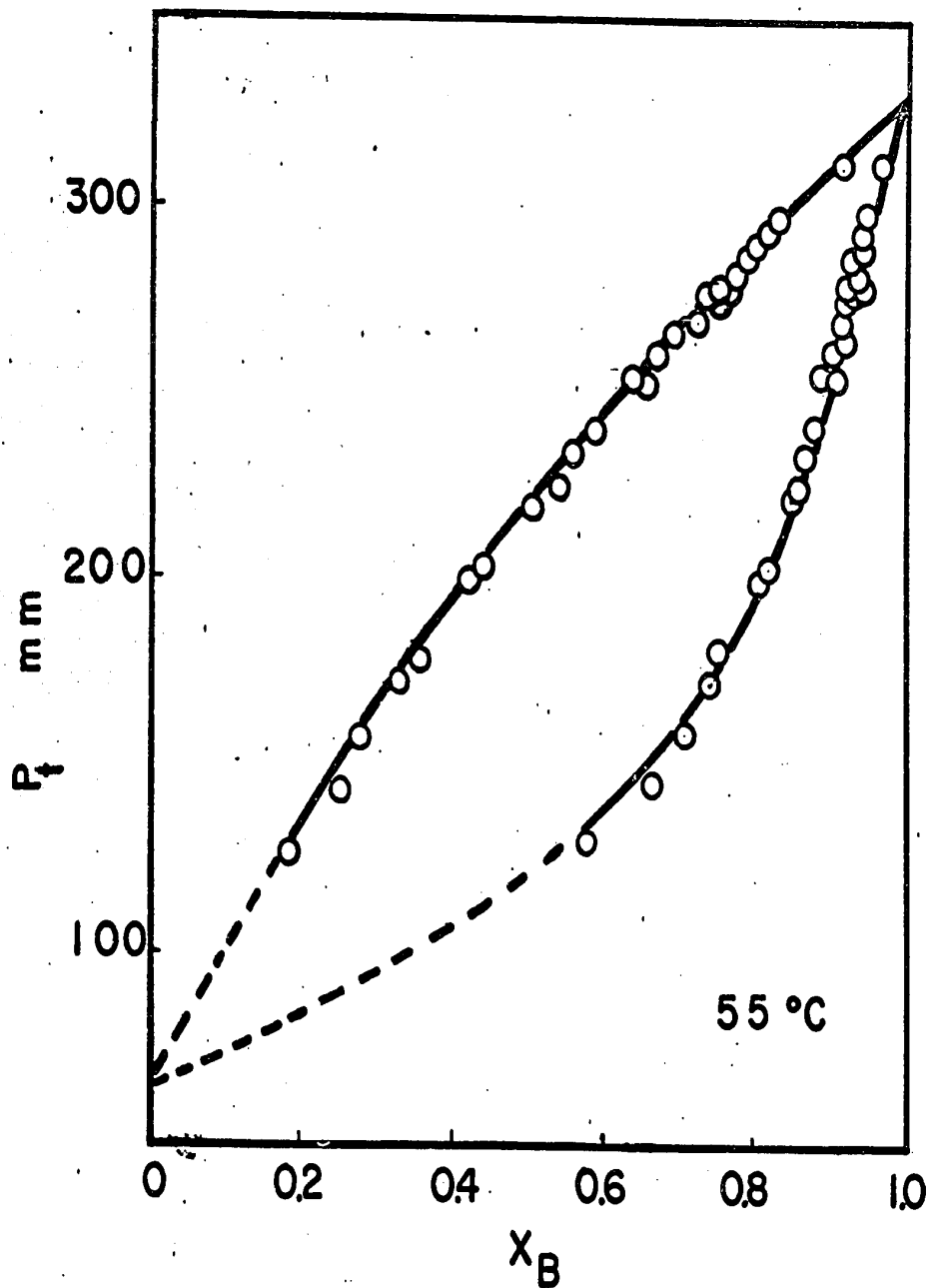


FIGURE 11: Total pressure - composition diagram for the system benzene (B) - n-octane (O) at 55°C.

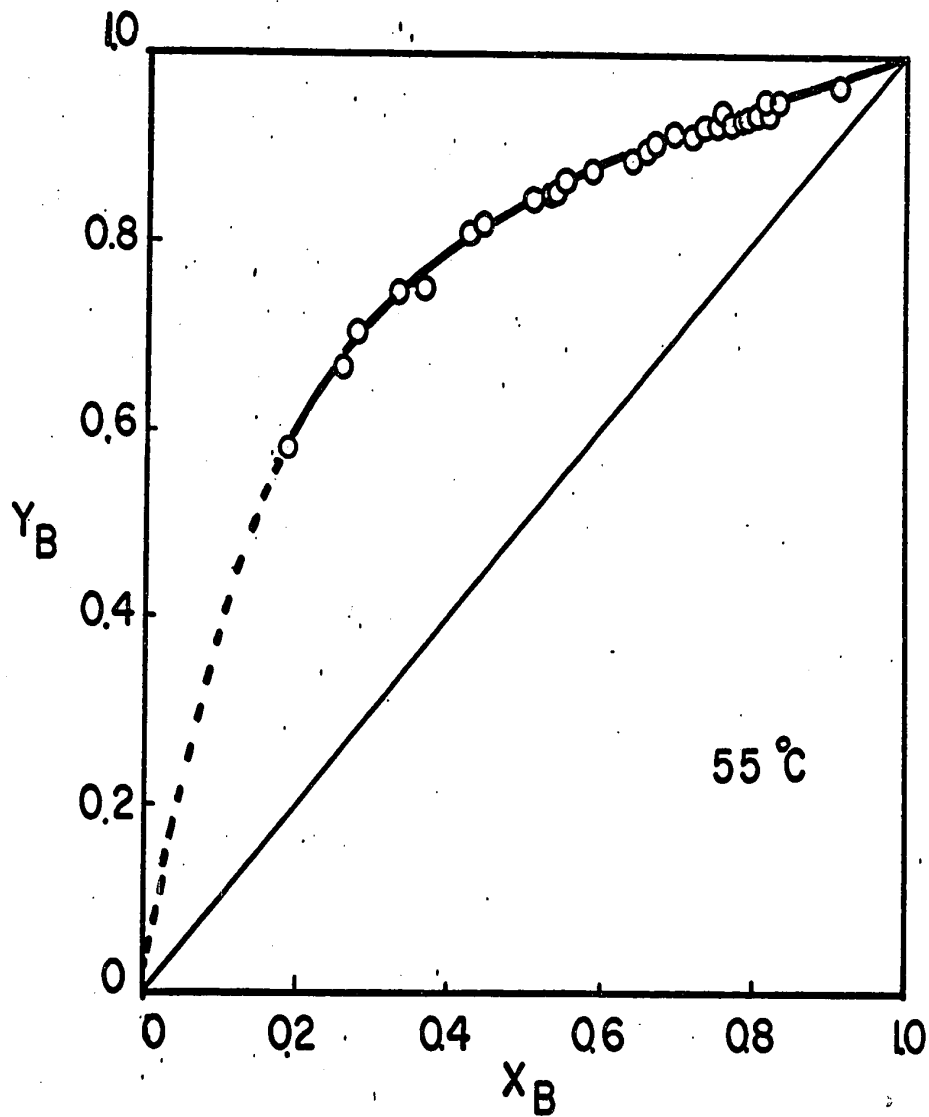


FIGURE 12: x - y curve for the system benzene (B) - n-octane (O) at 55°C.

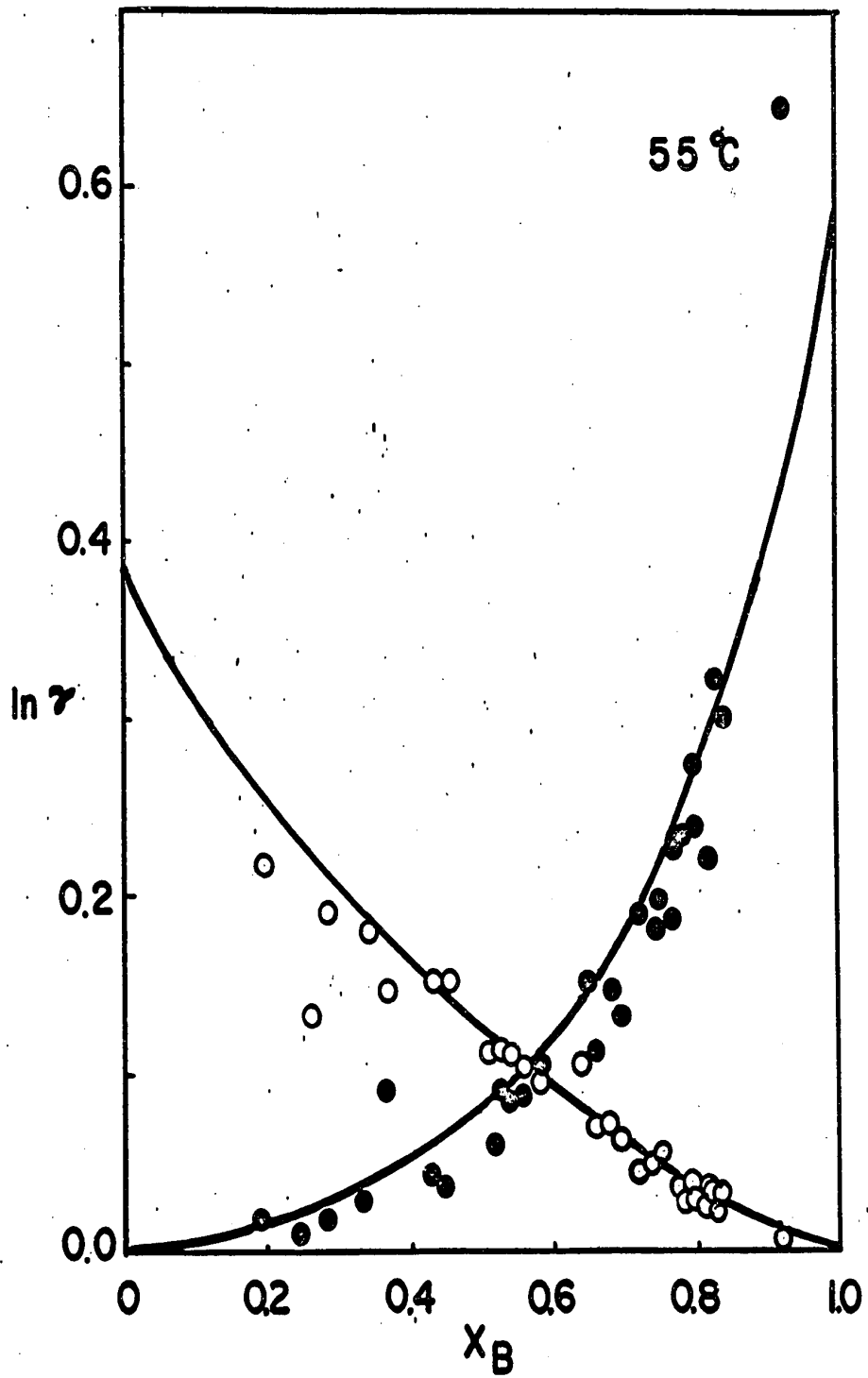


FIGURE 13: Activity coefficient vs. composition for benzene (B) -n-octane at 55° C.

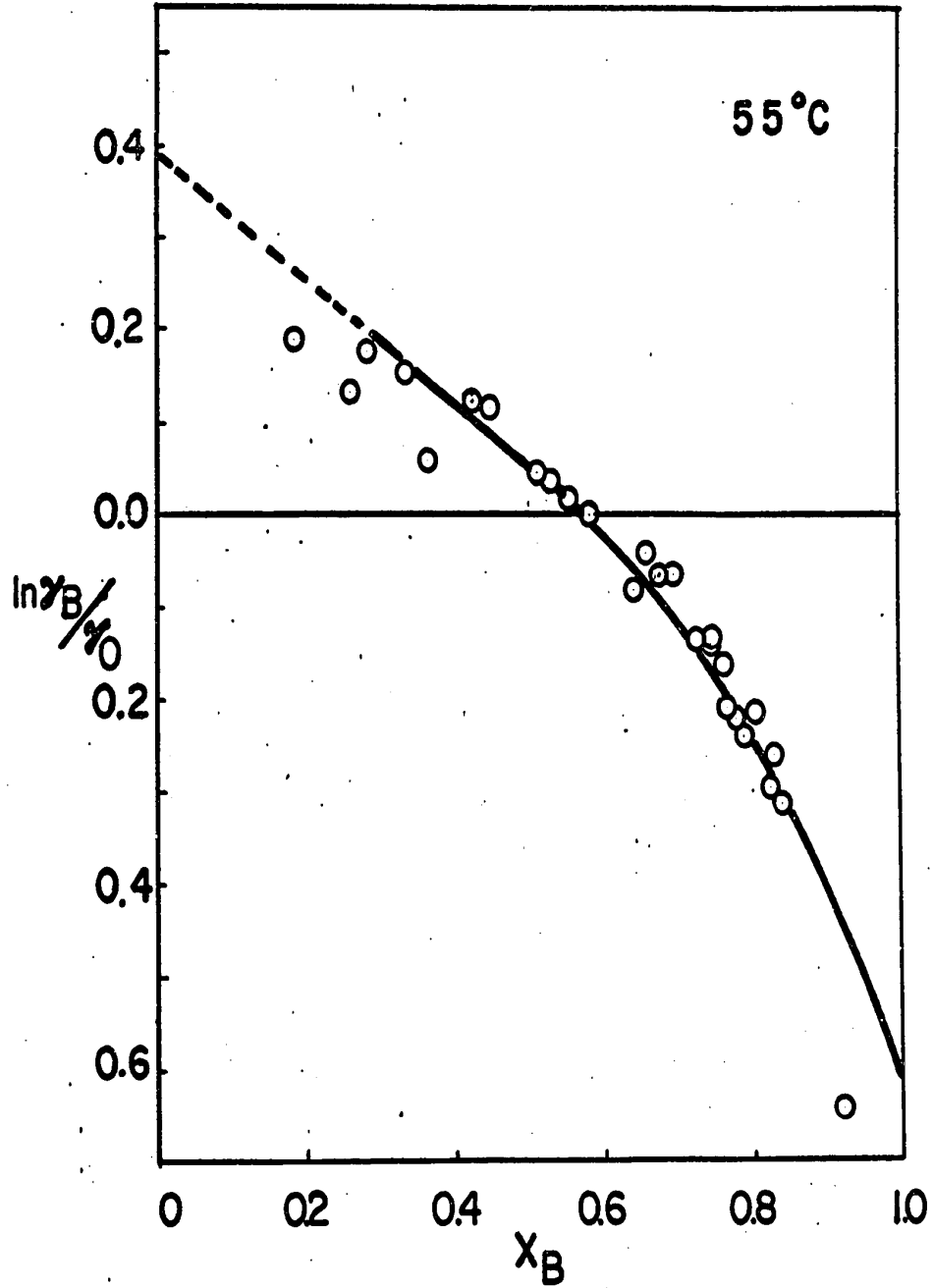


FIGURE 14: $\ln \gamma_B / \gamma_0$ - composition for the system benzene
(B) -n-octane (O) at 55°C.

VI DISCUSSION

1. The vapor pressure data for the pure components, at 75°C, 65°C, and 55°C, were calculated from the Antoine equation,

$$\log_{10} p = A - \frac{B}{C + t}$$

where,

p = vapor pressure of the pure component in m. m. Hg

A, B, C = constants

t = temperature in °C

For benzene, and n-octane the values of constants were taken from literature (41).

The second virial coefficients for benzene and n-octane were calculated from the equation proposed by Pitzer and Curl (30) using the following critical constants:

	<u>Benzene</u>	<u>n-octane</u>
$T_c, ^\circ K$	561.66	569.20
$P_c, \text{ atm}$	47.7	24.6

The values of the cross coefficient of benzene and n-octane were evaluated by the correlation given by O'Connell and Prausnitz (31).

The liquid molar volumes of benzene and n-octane at isothermal conditions of 75°C, 65°C and 55°C, were taken from the data by Young (42) and shown in Figure (17) and (18).

All values of vapor pressure, molar volume, second virial coefficient, and cross coefficient are listed in Table (5).

2. By comparing the values of $\ln \gamma$, obtained in this work at 75°C, and those obtained at the same isothermal condition for the system benzene-n-heptane ⁽⁴⁰⁾. It was observed that, as the chain length of the paraffinic hydrocarbon molecule increases, $\ln \gamma$ increases i.e. non-ideality increases.

An activity coefficient vs. composition diagram for the system benzene-n-heptane at 75°C is given in the appendix Figure (19).

3. From the results obtained in this work we get this table:

<u>Temperature °C</u>	<u>$(\ln \gamma_B)_{x_B = 0}$</u>	<u>$(\ln \gamma_0)_{x_B = 1}$</u>
75	0.2725	0.4721
65	0.3234	0.5514
55	0.3924	0.6112

It is seen, from the above table, that the activity coefficients at infinite dilution decrease with temperature, i.e. the heat of mixing is a positive quantity, which is in agreement with that of Lu ⁽⁴³⁾⁽⁴⁴⁾.

4. Reliability of experimental results:

For the three isotherms of the binary system benzene-n-octane 75°C, 65°C and 55°C, the net area of $\ln \gamma_1/\gamma_2$ vs. composition are as follows:

<u>Temperature °C</u>	<u>Area</u>
75	0.0001
65	0.0020
55	0.0030

The evaluated Redlich-Kister constants, fit the experimental data reasonably well as illustrated in Figure (6)(10)(14).

Hence it may be concluded that the experimental data are thermodynamically consistent.

5. Due to the difficulties involved in obtaining low pressures, the author was unable to obtain experimental data near the pure n-octane region.

VII CONCLUSIONS

1. Vapor-liquid equilibrium data obtained for the three isotherms 75°C, 65°C, and 55°C are thermodynamically consistent.
2. The Redlich-Kister constants determined from the experimental data are as follows:

<u>Temperature °C</u>	<u>B₁₂</u>	<u>C₁₂</u>	<u>D₁₂</u>
75	0.3222	0.0999	0.0500
65	0.3639	0.1140	0.0735
55	0.4202	0.1094	0.0816

VIII NOMENCLATURE

A, B, C	= constants of Antoine equation
B_{ii}	= second virial coefficient of pure component i in the equation of state
B_{12}, C_{12}, D_{12}	= constants of Redlich-Kister equations in the binary system
f	= fugacity
P	= total pressure
P_c	= critical pressure
p	= vapor pressure
Q	= $\frac{\Delta G^E}{2.303 RT}$ = Excess free energy function
R	= gas constant
T	= absolute temperature
T_c	= critical temperature
t	= temperature °C
V	= molar volume
x	= mole fraction in the liquid phase
y	= mole fraction in the vapor phase
$\ln f_1$	= $\exp. \left[\frac{(P - P_1)(B_{ii} - V_1)}{RT} + \frac{P^0 (1 - y_1)^2}{RT} \right]$
Z	= compressibility

GREEK LETTERS

v	= Residual volume
γ	= activity coefficient
ϕ	= fugacity coefficient of mixture
ϕ_i	= fugacity of component i in solution
δ_{12}	= cross coefficient of component 1 and 2

SUPERSCRIP TS

- L = liquid phase
- V = vapor phase
- 0 = standard state
- ^ = component i in solution

SUBSCRIPTS

- 1 = component 1
- 2 = component 2
- 1 2 = component 1 and 2
- i = component i

HEAD

IX REFERENCES

1. Redlich, O., and Kister, A. T., Ind., Eng. Chem. 40, 345 (1948).
2. Pierotti, G. J., C. H. Deal, and E. L. Derr, Ind., Eng. Chem., 51, 95 (1959).
3. Barker, J. A., J. Chem. Phys., 20, 1526 (1952).
4. Margules, M., Ann. Akad. Wiss. Wien., Math-naturw Kl., 104 (II): 1243, (1895).
5. Van Laar, J.; Z. Physik, Chem., 72, 723 (1910).
6. Scatchard, G. and W. Hamer; J. Am. Chem. Soc., 57, 1805 (1935).
7. Nerrish, R. S. and G. H. Twigg, Ind. Eng. Chem., 46, 201 (1954).
8. Gilmont, R., Ind. Eng. Chem., 42, 1907 (1950).
9. Gilmont, R., E. A. Weisman, F. Kramer, E. Miller, F. Hashmall, and D. F. Othmer, Ind. Eng. Chem., 42, 120 (1950).
10. Hirati, M., Japan Sci. Rev., 2 (3), 265 (1952).
11. Gillespie, D. T. C., Ind. Eng. Chem. Anal. Ed., 18, 575 (1946).
12. Redlich, O., Kister, A. T., and Turnquist, A. T., Chem. Eng. Progr., Symposium Ser. 1952, No. 2, 48, 49.
13. Jost, W. and Sieg, L. FIAT Report 1947, No. 1095, Data Compiled by Chu, J. C., "Vapor-Liquid Equilibrium Data", 1956 (Ann Arbor, Mich., J. W. Edwards Publishers Inc.).
14. Carney, T. P., "Laboratory Fractional Distillation", The Macmillan Co., New York, 1949.
15. Boerner and Johnson, Can. J. Research, 16B, 328 (1938).
16. Dodge and Dunbar, J. Am. Chem. Soc., 49, 591 (1927).
17. Freeth, and Verschoyle, Proc. Royal Soc. (London), A130, 453 (1931).

18. Verechyle, Trans. Roy. Soc. (London), A320, 189 (1931).
19. Callagart and Hitchcock, J. Am. Chem. Soc., 49, 750 (1927).
20. Cummings, Ind. Eng. Chem., 23, 900 (1931).
21. Kay, Ind. Eng. Chem., 30, 459 (1938).
22. Sage and Lacey, Eng. Ing. Chem., 26, 103 (1934).
23. Dobson, J. Chem. Soc., 127, 2866 (1925).
24. Odorff and Carrell, J. Phys. Chem., 1, 753 (1897).
25. Ringault, Ann. Chem., et Phys., (3) 15, 129 (1895).
26. Othmer, D. F., Ind. Eng. Chem., 20, 143 (1928).
27. Jones, C. A., Schoenborn, E. M., and Colburn, A. P., Ind. Eng. Chem., 35, 666 (1943).
28. Ellis, S. R. M., and Froome, B. A., Chem. and Ind., 237 (1954).
29. Cottrell, F. G., J. Am. Chem. Soc., 41, 721 (1919).
30. Pitzer, K. S., Curl, R. F., J. Am. Chem. Soc., 79, 2369, (1957).
31. O'Connell, J. P., and Prausnitz, J. M. Ind. Eng. Chem. Fund. ed., 6, 245 (1967).
32. Ho, J. C. K., Beahro, and B. C.-Y. Lu, Cand. J. Chem. Eng., 39, 205 (1961).
33. Driesback, R. R., "Physical Properties of Chemical Substances" Dow Chem. Co., Midland, Mich., (1952).
34. Fowler, R. T., Ind. Eng. Chem. Mfr., 24, 714 (1948).
35. Yuan, K. S., M. Sc. Thesis, Univ. of Ottawa (1961).
36. Otaki, H., and Williams, C. F., Chem. Eng. Progress Symp. Series, 49 No. 655 (1953).

37. S., Jean, Fu, M.Sc. Thesis, Univ. of Ottawa (1966).
38. Brown, L., Aust. J. Sci. Res., A5, 530 (1952).
39. Myers, H. S., Ind. Eng. Chem., 47, 2215 (1955).
40. Lu, B. C.-Y., S. Jean, Fu, J. Appl. Chem., Vol. 16 (1966).
41. Jordan, T. E., "Vapor Pressure of Organic Compounds", Interscience Publishers Inc., New York 1954.
42. Timmermans, J., "Physico-Chemical Constants of Pure Organic Compounds", Elsevier Publishing Co., Inc., (1950).
43. Lu, B. C.-Y., Cand. J. Chem. Eng., Octb., 193 (1959).
44. Lu, B. C.-Y., ibd. Feb., 22 (1967).

.81
.91
.02
.15
.35
.55
.65
.75
.85
.95
)
.10
.20
.30
.40
.50
.60
.70
.80
.90
.00

X - APPENDIX I

TABLE (3)

Calibration of Temperature - Absolute Millivolts
for the Iron - Constantan Thermocouple

	<u>Temperature °C</u>	<u>e. m. f. absolute millivolts</u>
1	34.740	1.7504
2	36.240	1.8303
3	37.765	1.9113
4	42.370	2.1602
5	44.710	2.2859
6	46.770	2.3948
7	48.020	2.4623
8	55.125	2.8535
9	56.040	2.9249
10	76.810	4.0206
11	80.229	4.1944
12	98.428	5.2125

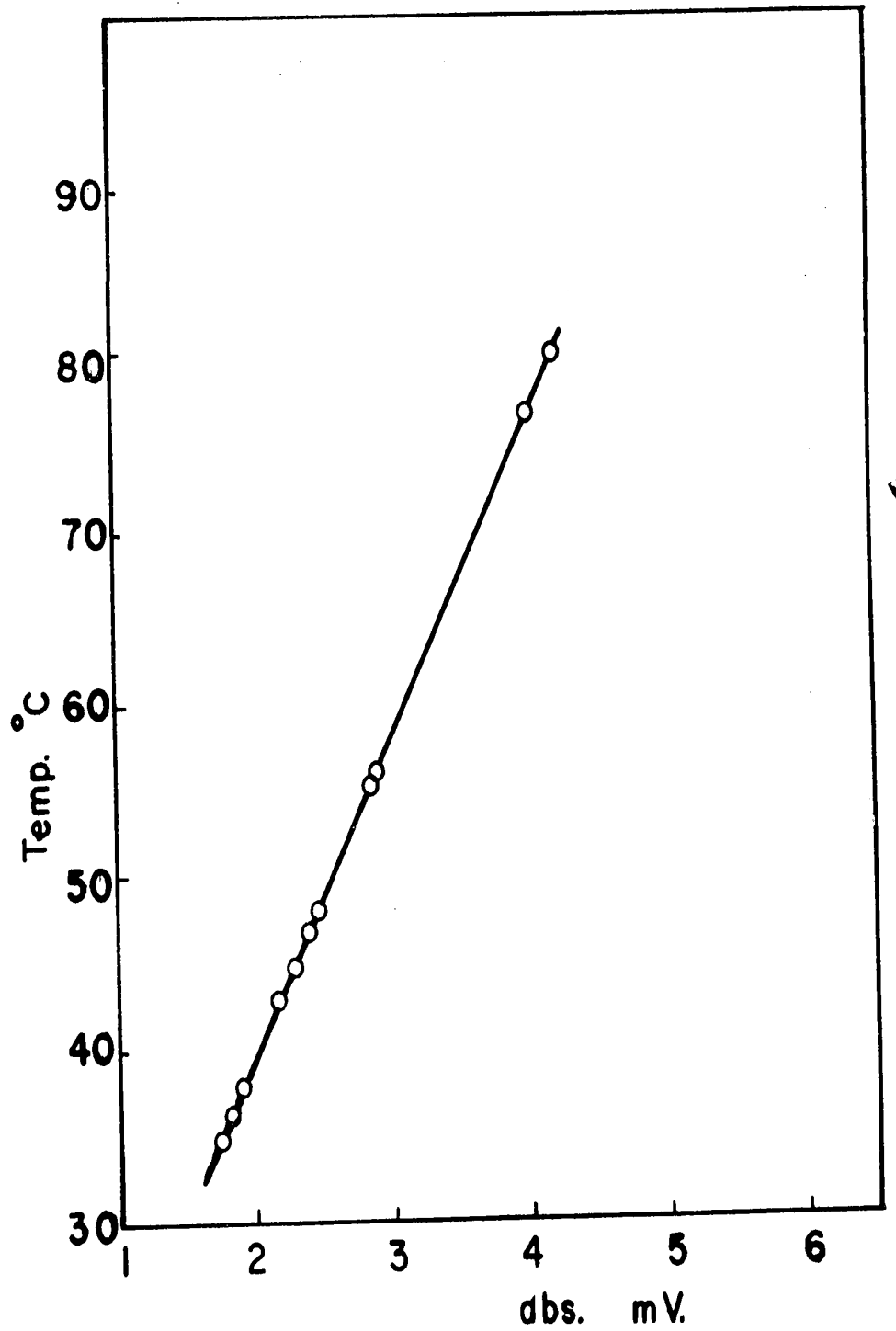


FIGURE 15: Calibration of Fe - constantan thermocouple.

TABLE (4)

Calibration of Composition - Refractive Index for
the System Benzene-n-Octane

<u>Run</u>	<u>Mole fraction of benzene x_1</u>	<u>Refractive index at 25° C</u>
1	0	1.39513
2	0.0419	1.39711
3	0.0998	1.40024
4	0.1178	1.40108
5	0.2016	1.40620
6	0.2770	1.41093
7	0.4247	1.42185
8	0.4745	1.42601
9	0.5147	1.42961
10	0.5195	1.42995
11	0.5925	1.43694
12	0.6237	1.44031
13	0.6491	1.44326
14	0.6974	1.44945
15	0.7023	1.45313
16	0.7314	1.45394
17	0.7380	1.45881
18	0.7739	1.47603
19	0.8859	1.48056
20	0.9116	1.48290
21	0.9245	1.49213
22	0.9718	1.49801
23	1.0000	1.49790

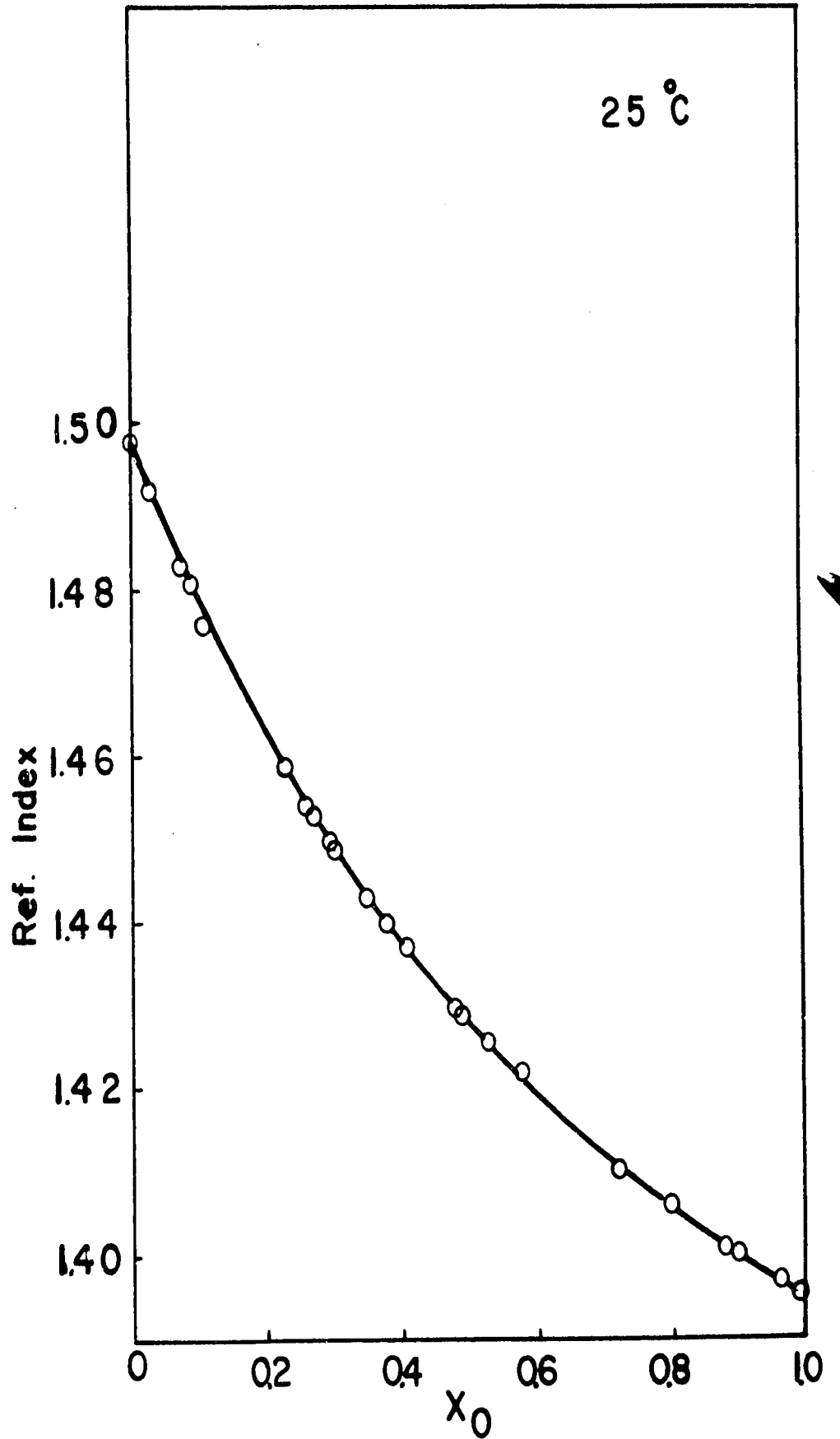


FIGURE 16: Calibration curve of composition - refractive index for the system benzene-n-octane at 25° C.

TABLE (5)

Second Virial Coefficients, Cross Coefficients,
and Molar Volumes

AT 75° C

	<u>B_{11} (cc/mol)</u>	<u>δ_{12} (cc/mol)</u>	<u>V_i^L (cc/mol)</u>
Benzene (1)	- 949.9331		95.2852
		+ 173.8600	
n-octane (2)	- 2099.1787		173.9099

AT 65° C

Benzene (1)	- 1009.1259		94.0608
		+ 186.7497	
n-octane (2)	- 2237.2549		171.7422

AT 55° C

Benzene (1)	- 1073.8093		92.8679
		+ 200.9562	
n-octane (2)	- 2388.6404		169.6102

TABLE (6)

**Redlich-Kister Constants for the Three Isotherms of the Binary
System Benzene-n-Octane**

Temperature °C	B₁₂	C₁₂	D₁₂
75	0.3222	0.0999	0.0500
65	0.3639	0.1140	0.0735
55	0.4202	0.1094	0.0816

TABLE (7)

Liquid Density of Benzene at Various Temperatures (42)

<u>Temperature</u> <u>°C</u>	<u>Density</u> <u>gm/cc</u>
0	0.90006
10	0.8895
20	0.8790
30	0.8685
40	0.8576
50	0.8466
60	0.8357
70	0.8248
80	0.8145

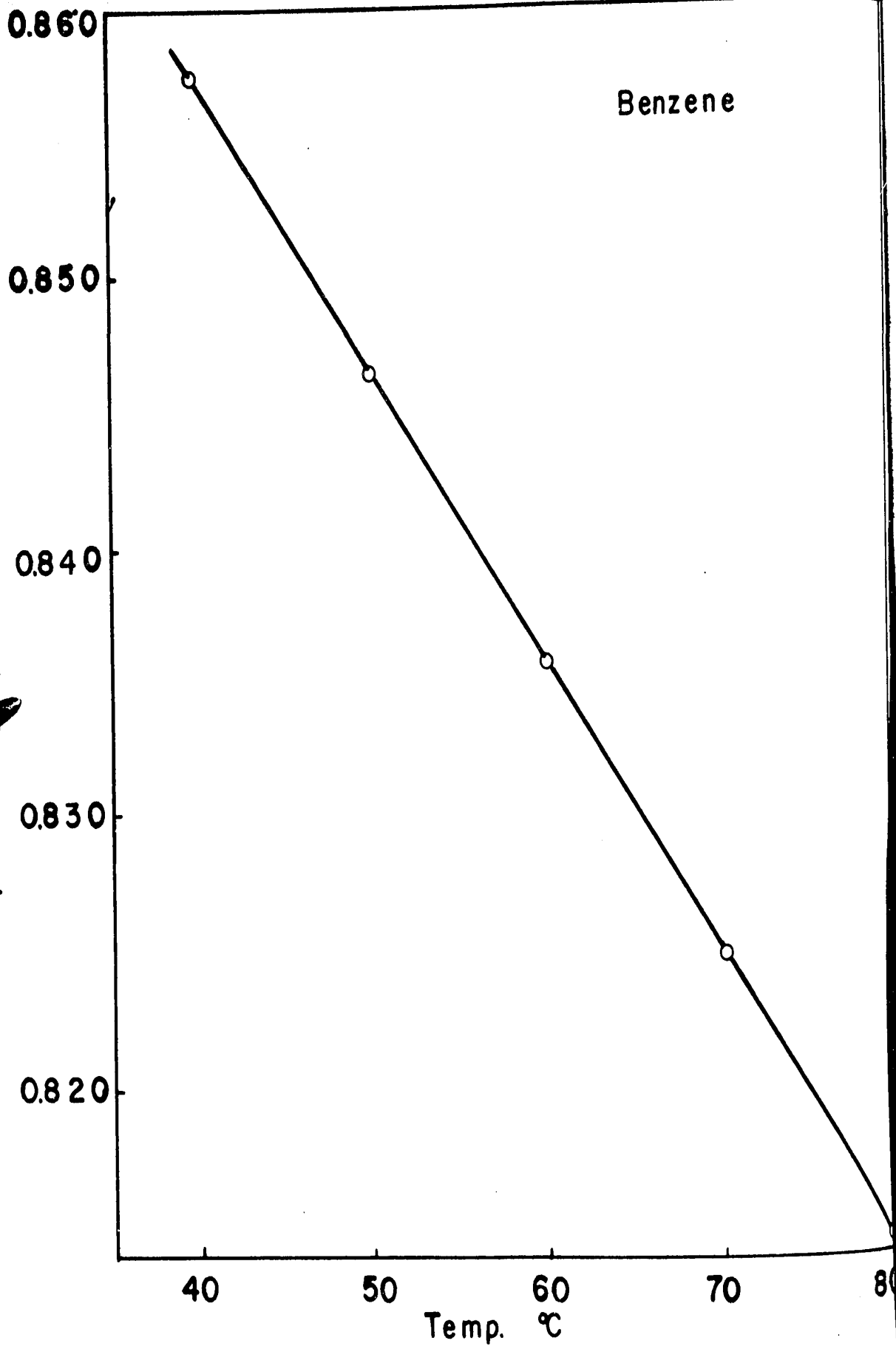


FIGURE 17: Density of liquid benzene-temperature curve.

TABLE (8)

Liquid Density of n-Octane at Various Temperature (42)

<u>Temperature °C</u>	<u>Density gm/cc</u>
0	0.71848
10	0.71020
20	0.7022
30	0.6942
40	0.6860
50	0.6778
60	0.6694
70	0.6611
80	0.6525

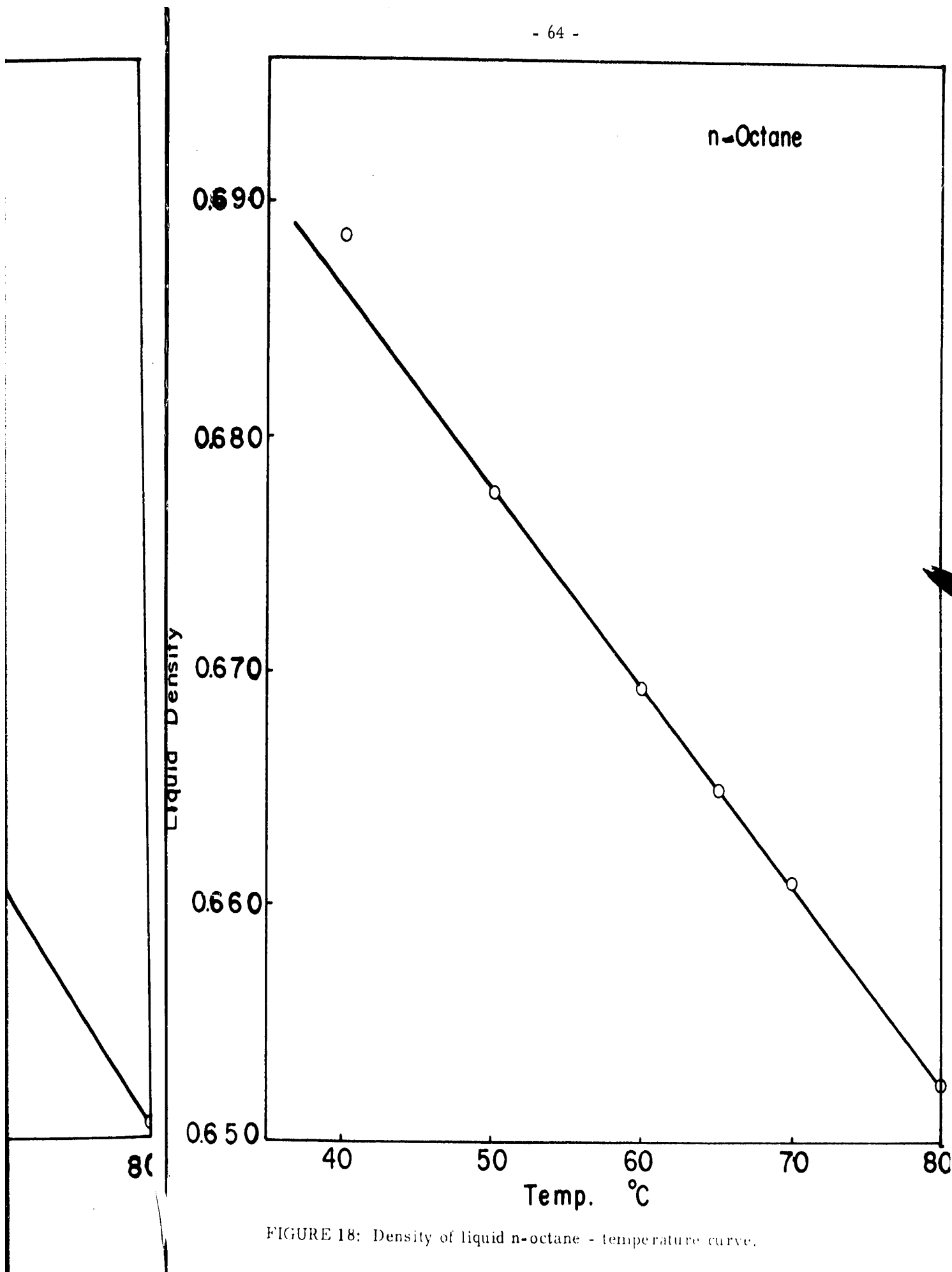


FIGURE 18: Density of liquid n-octane - temperature curve.

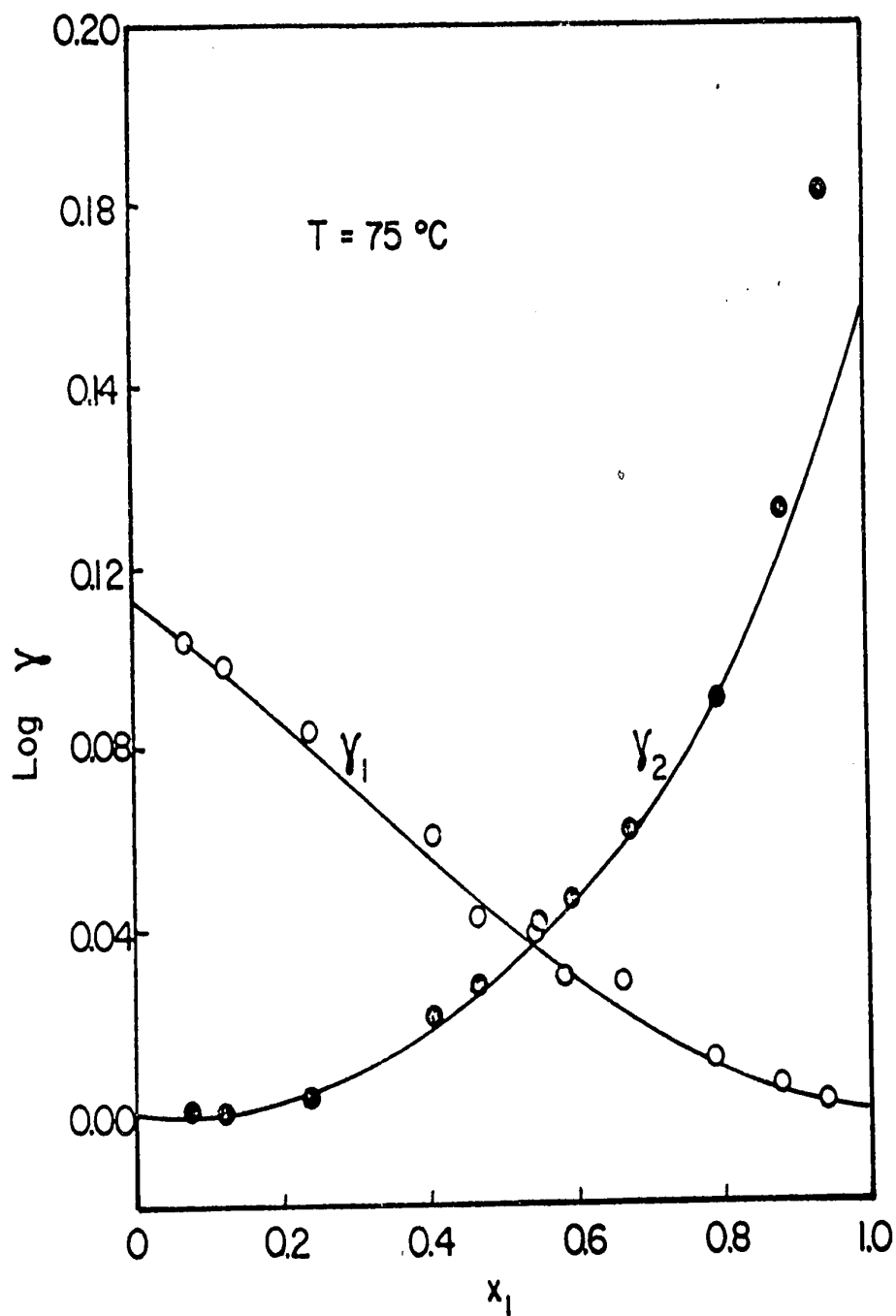


Figure 19. Activity coefficients vs. composition diagram for the system benzene(1)-n-heptane(2) at 75°C

XI - APPENDIX II

SAMPLE CALCULATIONS

1. Calculation of mole fraction of the sample

This is done using the calibration curve Figure (16).

2. Evaluation of Z''_B values

Using table (2) Run (5)

$$\text{Since } Z''_B = \frac{(P_t - P_B) (B_{BB} - V_B^L)}{RT}$$

$$P_t = 502.71 \text{ mm.}$$

$$P_B = 648.34 \text{ mm.}$$

$$B_{BB} = -949.9331 \text{ (cc/mol)}$$

$$V_B^L = 95.2851 \text{ cc/mol}$$

$$Z''_B = \frac{(502.71 - 648.34) (-949.9331 - 95.2851)}{760 \times 82.0567 \times 348}$$
$$= 0.0070$$

By similar procedure Z''_0 can be calculated.

3. Evaluation of δ_B and δ_0

Using table (2) Run (5)

$$\text{Since } \delta_B = \left(\frac{P_t \delta_{0B}}{RT} \right) y_0^2$$

$$y_0 = (1 - 0.8850) = 0.1150$$

$$\delta_{0B} = 173.8600 \text{ cc/mol}$$

$$\delta_B = \left(\frac{502.71 \times 173.8600}{760 \times 82.0567 \times 348} \right) (0.1150)^2$$

$$= 0.0001$$

Similarly δ_0 can be calculated.

4. Evaluation of liquid phase activity coefficients

Using table (2) Run (5)

$$\text{Since } \ln \gamma_B = \ln \frac{P_t y_B}{P_B x_B} + Z''_B + \delta_B$$

where,

$$Z'_i = e^{(Z''_i + \delta_i)}$$

$$\ln \gamma_B = \ln \left(\frac{502.71 \times 0.8850}{648.34 \times 0.6505} \right) + 0.00701 + 0.0005$$

$$= 0.0534 + 0.00701 + 0.00005$$

$$= 0.06046 \approx 0.06050$$

5. Determination of Binary Redlich-Kister Constants

The constants B_{12} , C_{12} and D_{12} are determined by the method of least square fit, using digital computer IBM 360-40.

The mathematics involved are as follows:

Since,

$$\ln \left(\frac{y_1}{y_2} \right) = B (1 - x_1) + C (6x_1 x_2 - 1) + D (1 - 2x_1)$$

$$(1 - 8x_1 x_2) \dots \dots \dots (1)$$

$$y_{\text{obs.}} = B Z_1 + C Z_2 + D Z_3 \dots \dots \dots (2)$$

where,

$$y_{\text{obs}} = \ln\left(\frac{y_1}{y_2}\right)$$

$$Z_1 = (1 - x_1)$$

$$Z_2 = (6x_1 x_2 - 1)$$

$$Z_3 = (1 - 2x_1) (1 - 8x_1 x_2)$$

Let,

$$S = \sum_{i=1}^n (\Delta y)^2$$
$$= \sum_{i=1}^n \left[y_{\text{obs}} - (BZ_1 + CZ_2 + DZ_3) \right]^2 \dots\dots (3)$$

n = number of observations

Partial differentiation of equation (3) with respect to B, C, and D respectively gives,

$$\frac{\partial S}{\partial B} = 2 \sum_{i=1}^n \left[y_{\text{obs}} - (BZ_1 + CZ_2 + DZ_3) \right] Z_1 \dots\dots\dots (4)$$

$$\frac{\partial S}{\partial C} = 2 \sum_{i=1}^n \left[y_{\text{obs}} - (BZ_1 + CZ_2 + DZ_3) \right] Z_2 \dots\dots\dots (5)$$

$$\frac{\partial S}{\partial D} = 2 \sum_{i=1}^n \left[y_{\text{obs}} - (BZ_1 + CZ_2 + DZ_3) \right] Z_3 \dots\dots\dots (6)$$

Minimizing S by setting $\frac{\partial S}{\partial B}$, $\frac{\partial S}{\partial C}$, and $\frac{\partial S}{\partial D}$ equal to zero
 Equations (4), (5) and (6) will be as follows,

$$\sum_{i=1}^n (BZ_1 + CZ_2 + DZ_3) Z_1 = \sum_{i=1}^n y_{obs.} Z_1 \dots\dots\dots (7)$$

$$\sum_{i=1}^n (BZ_1 + CZ_2 + DZ_3) Z_2 = \sum_{i=1}^n y_{obs.} Z_2 \dots\dots\dots (8)$$

$$\sum_{i=1}^n (BZ_1 + CZ_2 + DZ_3) Z_3 = \sum_{i=1}^n y_{obs.} Z_3 \dots\dots\dots (9)$$

Expanding equations (7), (8) and (9) to give the normalized equations,

$$\sum_{i=1}^n y_{obs.} Z_1 = B \sum_{i=1}^n Z_1^2 + C \sum_{i=1}^n Z_1 Z_2 + D \sum_{i=1}^n Z_1 Z_3$$

\dots\dots\dots(10)

$$\sum_{i=1}^n y_{obs.} Z_2 = B \sum_{i=1}^n Z_1 Z_2 + C \sum_{i=1}^n Z_2^2 + D \sum_{i=1}^n Z_2 Z_3$$

\dots\dots\dots(11)

$$\sum_{i=1}^n y_{obs.} Z_3 = B \sum_{i=1}^n Z_1 Z_3 + C \sum_{i=1}^n Z_2 Z_3 + D \sum_{i=1}^n Z_3^2$$

\dots\dots\dots(12)

By solving equations (10), (11) and (12) simultaneously B, C, and D can be obtained.

```

C LEAST SQUARE CURVE FITTING TO THE REDLISH-KISTER EQU OF THREE CONSTANTS
C DR .LJ (DEPT OF CHEM. ENG.)
DIMENSION GAMMA(50), GAMMA(50), A(10,11)
DIMENSION P(50), X(50), Y(50), GI(50), GT(50)
DIMENSION TITL(80)
1 READ(1,102) TITL(1), I=1,80)
102 FORMAT(180A1)
DO 10 J=1,10
DO 10 J=1,11
AT(J,J)=0.0
WRITE(3,103) TITL(1), I=1,80)
103 FORMAT(14,80A1)
READ(1,101) N,NRS,NEQ
101 FORMAT(2I3)
DO 20 I=1,NRS
READ(1,100) P(I), X(I), Y(I), GI(I), GT(I)
WRITE(3,104) P(I), X(I), Y(I), GI(I), GT(I)
FORMAT(F10.2)
100 FORMAT(F10.2)
11 GT(I)=1./EXP(-GI(I))
12 GT(I)=1.0
13 GI(I)=EXP(GI(I))
14 YE(GI(I))=15.16,17
15 YE(GI(I))=1.0/EXP(-GI(I))
16 GT(I)=1.0
17 G(T)=EXP(G(T))
18 CONTINUE
F=1.-2.*Y(T)
G=X(I)*I.-X(I)
H=4.*G-1.
C=1.-R.*G
F=ALNG(G(T)/G(Y(T)))
A(1,1)=A(1,1)+E*F
A(1,2)=A(1,2)+E*H
A(1,3)=A(1,3)+E*F*G
A(1,4)=A(1,4)+E*F*H
A(2,2)=A(2,2)+H*H
A(2,3)=A(2,3)+F*H*G
A(2,4)=A(2,4)+H*F
A(3,3)=A(3,3)+F*F*G*G
A(3,4)=A(3,4)+F*F*G*F
CONTINUE
A(2,1)=A(1,2)
A(3,1)=A(1,3)
A(3,2)=A(2,3)
CALL SOLVE(NEG,A,INDIC)
NFOI=NEQ+1
WRITE(3,105) (A(I),NEG(I),I=1,NEQ)

```

